Nonlinear Systems

Hassan K. Khalil

Third Edition

Pearson New International Edition

PEARSON®

Pearson New International Edition

Nonlinear Systems

Hassan K. Khalil
Third Edition

PEARSON®

Pearson Education Limited
Edinburgh Gate
Harlow
Essex CM20 2JE
England and Associated Companies throughout the world

Visit us on the World Wide Web at: www.pearsoned.co.uk

PEARSON®

ISBN 10: 1-292-03921-3
ISBN 13: 978-1-292-03921-3

British Library Cataloguing-in-Publication Data
A catalogue record for this book is available from the British Library

Printed in the United States of America

Table of Contents

Chapter 1

Introduction

When engineers analyze and design nonlinear dynamical systems in electrical circuits, mechanical systems, control systems, and other engineering disciplines, they need to absorb and digest a wide range of nonlinear analysis tools. In this book, we introduce some of the these tools. In particular, we present tools for the stability analysis of nonlinear systems, with emphasis on Lyapunov's method. We give special attention to the stability of feedback systems from input–output and passivity perspectives. We present tools for the detection and analysis of "free" oscillations, including the describing function method. We introduce the asymptotic tools of perturbation theory, including averaging and singular perturbations. Finally, we introduce nonlinear feedback control tools, including linearization, gain scheduling, integral control, feedback linearization, sliding mode control, Lyapunov redesign, backstepping, passivity-based control, and high-gain observers.

1.1 Nonlinear Models and Nonlinear Phenomena

We will deal with dynamical systems that are modeled by a finite number of coupled first-order ordinary differential equations

$$\begin{aligned}
\dot{x}_1 &= f_1(t, x_1, \ldots, x_n, u_1, \ldots, u_p) \\
\dot{x}_2 &= f_2(t, x_1, \ldots, x_n, u_1, \ldots, u_p) \\
\vdots \quad &\quad \vdots \\
\dot{x}_n &= f_n(t, x_1, \ldots, x_n, u_1, \ldots, u_p)
\end{aligned}$$

where $\dot{x}_i$ denotes the derivative of x_i with respect to the time variable t and u_1, u_2, $\ldots$, u_p are specified input variables. We call the variables x_1, x_2, $\ldots$, x_n the state variables. They represent the memory that the dynamical system has of its past.

From Chapter 1 of *Nonlinear Systems*, Third Edition. Hassan K. Khalil.

We usually use vector notation to write these equations in a compact form. Define

$$x = \begin{bmatrix} x_1 \\ x_2 \\ \vdots \\ \vdots \\ x_n \end{bmatrix}, \quad u = \begin{bmatrix} u_1 \\ u_2 \\ \vdots \\ u_p \end{bmatrix}, \quad f(t,x,u) = \begin{bmatrix} f_1(t,x,u) \\ f_2(t,x,u) \\ \vdots \\ \vdots \\ f_n(t,x,u) \end{bmatrix}$$

and rewrite the n first-order differential equations as one n-dimensional first-order vector differential equation

$$\dot{x} = f(t,x,u) \tag{1.1}$$

We call (1.1) the state equation and refer to x as the *state* and u as the *input*. Sometimes, another equation

$$y = h(t,x,u) \tag{1.2}$$

is associated with (1.1), thereby defining a q-dimensional *output* vector y that comprises variables of particular interest in the analysis of the dynamical system, (e.g., variables that can be physically measured or variables that are required to behave in a specified manner). We call (1.2) the output equation and refer to equations (1.1) and (1.2) together as the state-space model, or simply the state model. Mathematical models of finite-dimensional physical systems do not always come in the form of a state model. However, more often than not, we can model physical systems in this form by carefully choosing the state variables. Examples and exercises that will appear later in the chapter will demonstrate the versatility of the state model.

A good part of our analysis in this book will deal with the state equation, many times without explicit presence of an input u, that is, the so-called unforced state equation

$$\dot{x} = f(t,x) \tag{1.3}$$

Working with an unforced state equation does not necessarily mean that the input to the system is zero. It could be that the input has been specified as a given function of time, $u = \gamma(t)$, a given feedback function of the state, $u = \gamma(x)$, or both, $u = \gamma(t,x)$. Substituting $u = \gamma$ in (1.1) eliminates u and yields an unforced state equation.

A special case of (1.3) arises when the function f does not depend explicitly on t; that is,

$$\dot{x} = f(x) \tag{1.4}$$

in which case the system is said to be *autonomous* or *time invariant*. The behavior of an autonomous system is invariant to shifts in the time origin, since changing the time variable from t to $\tau = t - a$ does not change the right-hand side of the state equation. If the system is not autonomous, then it is called *nonautonomous* or *time varying.*

An important concept in dealing with the state equation is the concept of an equilibrium point. A point $x = x^*$ in the state space is said to be an equilibrium point of (1.3) if it has the property that whenever the state of the system starts at x^*, it will remain at x^* for all future time. For the autonomous system (1.4), the equilibrium points are the real roots of the equation

$$f(x) = 0$$

An equilibrium point could be isolated; that is, there are no other equilibrium points in its vicinity, or there could be a continuum of equilibrium points.

For linear systems, the state model (1.1)–(1.2) takes the special form

$$\begin{aligned}\dot{x} &= A(t)x + B(t)u \\ y &= C(t)x + D(t)u\end{aligned}$$

We assume that the reader is familiar with the powerful analysis tools for linear systems, founded on the basis of the *superposition principle.* As we move from linear to nonlinear systems, we are faced with a more difficult situation. The superposition principle does not hold any longer, and analysis tools involve more advanced mathematics. Because of the powerful tools we know for linear systems, the first step in analyzing a nonlinear system is usually to linearize it, if possible, about some nominal operating point and analyze the resulting linear model. This is a common practice in engineering, and it is a useful one. There is no question that, whenever possible, we should make use of linearization to learn as much as we can about the behavior of a nonlinear system. However, linearization alone will not be sufficient; we must develop tools for the analysis of nonlinear systems. There are two basic limitations of linearization. First, since linearization is an approximation in the neighborhood of an operating point, it can only predict the "local" behavior of the nonlinear system in the vicinity of that point. It cannot predict the "nonlocal" behavior far from the operating point and certainly not the "global" behavior throughout the state space. Second, the dynamics of a nonlinear system are much richer than the dynamics of a linear system. There are "essentially nonlinear phenomena" that can take place only in the presence of nonlinearity; hence, they cannot be described or predicted by linear models. The following are examples of essentially nonlinear phenomena:

- *Finite escape time.* The state of an unstable linear system goes to infinity as time approaches infinity; a nonlinear system's state, however, can go to infinity in finite time.

- *Multiple isolated equilibria.* A linear system can have only one isolated equilibrium point; thus, it can have only one steady-state operating point that attracts the state of the system irrespective of the initial state. A nonlinear system can have more than one isolated equilibrium point. The state may converge to one of several steady-state operating points, depending on the initial state of the system.

- *Limit cycles.* For a linear time-invariant system to oscillate, it must have a pair of eigenvalues on the imaginary axis, which is a nonrobust condition that is almost impossible to maintain in the presence of perturbations. Even if we do, the amplitude of oscillation will be dependent on the initial state. In real life, stable oscillation must be produced by nonlinear systems. There are nonlinear systems that can go into an oscillation of fixed amplitude and frequency, irrespective of the initial state. This type of oscillation is known as a limit cycle.

- *Subharmonic, harmonic, or almost-periodic oscillations.* A stable linear system under a periodic input produces an output of the same frequency. A nonlinear system under periodic excitation can oscillate with frequencies that are submultiples or multiples of the input frequency. It may even generate an almost-periodic oscillation, an example is the sum of periodic oscillations with frequencies that are not multiples of each other.

- *Chaos.* A nonlinear system can have a more complicated steady-state behavior that is not equilibrium, periodic oscillation, or almost-periodic oscillation. Such behavior is usually referred to as chaos. Some of these chaotic motions exhibit randomness, despite the deterministic nature of the system.

- *Multiple modes of behavior.* It is not unusual for two or more modes of behavior to be exhibited by the same nonlinear system. An unforced system may have more than one limit cycle. A forced system with periodic excitation may exhibit harmonic, subharmonic, or more complicated steady-state behavior, depending upon the amplitude and frequency of the input. It may even exhibit a discontinuous jump in the mode of behavior as the amplitude or frequency of the excitation is smoothly changed.

In this book, we will encounter only the first three of these phenomena.[1] Multiple equilibria and limit cycles will be introduced in the next chapter, as we examine second-order autonomous systems, while the phenomenon of finite escape time will be introduced in Chapter 3.

[1] To read about forced oscillation, chaos, bifurcation, and other important topics, the reader may consult [70], [74], [187], and [207].

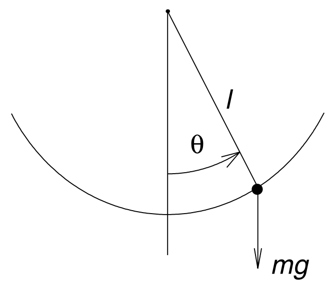

Figure 1.1: Pendulum.

1.2 Examples

1.2.1 Pendulum Equation

Consider the simple pendulum shown in Figure 1.1, where l denotes the length of the rod and m denotes the mass of the bob. Assume the rod is rigid and has zero mass. Let θ denote the angle subtended by the rod and the vertical axis through the pivot point. The pendulum is free to swing in the vertical plane. The bob of the pendulum moves in a circle of radius l. To write the equation of motion of the pendulum, let us identify the forces acting on the bob. There is a downward gravitational force equal to mg, where g is the acceleration due to gravity. There is also a frictional force resisting the motion, which we assume to be proportional to the speed of the bob with a coefficient of friction k. Using Newton's second law of motion, we can write the equation of motion in the tangential direction as

$$ml\ddot{\theta} = -mg\sin\theta - kl\dot{\theta}$$

Writing the equation of motion in the tangential direction has the advantage that the rod tension, which is in the normal direction, does not appear in the equation. We could have arrived at the same equation by writing the moment equation about the pivot point. To obtain a state model for the pendulum, let us take the state variables as $x_1 = \theta$ and $x_2 = \dot{\theta}$. Then, the state equations are

$$\dot{x}_1 = x_2 \tag{1.5}$$

$$\dot{x}_2 = -\frac{g}{l}\sin x_1 - \frac{k}{m}x_2 \tag{1.6}$$

To find the equilibrium points, we set $\dot{x}_1 = \dot{x}_2 = 0$ and solve for x_1 and x_2:

$$\begin{aligned} 0 &= x_2 \\ 0 &= -\frac{g}{l}\sin x_1 - \frac{k}{m}x_2 \end{aligned}$$

The equilibrium points are located at $(n\pi, 0)$, for $n = 0, \pm 1, \pm 2, \ldots$. From the physical description of the pendulum, it is clear that the pendulum has only two equilibrium positions corresponding to the equilibrium points $(0, 0)$ and $(\pi, 0)$. Other equilibrium points are repetitions of these two positions, which correspond to the number of full swings the pendulum would make before it rests at one of the two equilibrium positions. For example, if the pendulum makes m complete $360°$ revolutions before it rests at the downward vertical position, then, mathematically, we say that the pendulum approaches the equilibrium point $(2m\pi, 0)$. In our investigation of the pendulum, we will limit our attention to the two "nontrivial" equilibrium points at $(0, 0)$ and $(\pi, 0)$. Physically, we can see that these two equilibrium positions are quite distinct from each other. While the pendulum can indeed rest at the $(0, 0)$ equilibrium point, it can hardly maintain rest at the $(\pi, 0)$ equilibrium point because infinitesimally small disturbance from that equilibrium will take the pendulum away. The difference between the two equilibrium points is in their stability properties, a topic we will study in some depth.

Sometimes it is instructive to consider a version of the pendulum equation where the frictional resistance is neglected by setting $k = 0$. The resulting system

$$\dot{x}_1 = x_2 \tag{1.7}$$

$$\dot{x}_2 = -\frac{g}{l}\sin x_1 \tag{1.8}$$

is conservative in the sense that if the pendulum is given an initial push, it will keep oscillating forever with a nondissipative energy exchange between kinetic and potential energies. This, of course, is not realistic, but gives insight into the behavior of the pendulum. It may also help in finding approximate solutions of the pendulum equation when the friction coefficient k is small. Another version of the pendulum equation arises if we can apply a torque T to the pendulum. This torque may be viewed as a control input in the equation

$$\dot{x}_1 = x_2 \tag{1.9}$$

$$\dot{x}_2 = -\frac{g}{l}\sin x_1 - \frac{k}{m}x_2 + \frac{1}{ml^2}T \tag{1.10}$$

Interestingly enough, several unrelated physical systems are modeled by equations similar to the pendulum equation. Such examples are the model of a synchronous generator connected to an infinite bus (Exercise 1.8), the model of a Josephson junction circuit (Exercise 1.9), and the model of a phase-locked loop (Exercise 1.11). Consequently, the pendulum equation is of great practical importance.

1.2.2 Tunnel-Diode Circuit

Consider the tunnel-diode circuit shown in Figure 1.2,[2] where the tunnel diode is characterized by $i_R = h(v_R)$. The energy-storing elements in this circuit are the

[2]This figure, as well as Figures 1.3 and 1.7, are taken from [39].

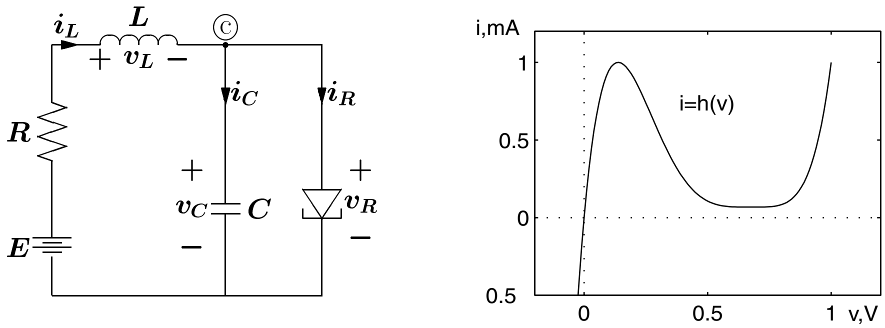

(a) (b)

Figure 1.2: (a) Tunnel-diode circuit; (b) Tunnel-diode v_R–i_R characteristic.

capacitor C and the inductor L. Assuming they are linear and time invariant, we can model them by the equations

$$i_C = C\frac{dv_C}{dt} \quad \text{and} \quad v_L = L\frac{di_L}{dt}$$

where i and v are the current through and the voltage across an element, with the subscript specifying the element. To write a state model for the system, let us take $x_1 = v_C$ and $x_2 = i_L$ as the state variables and $u = E$ as a constant input. To write the state equation for x_1, we need to express i_C as a function of the state variables x_1, x_2 and the input u. Using Kirchhoff's current law, we can write an equation that the algebraic sum of all currents leaving node ⓒ is equal to zero:

$$i_C + i_R - i_L = 0$$

Therefore,

$$i_C = -h(x_1) + x_2$$

Similarly, we need to express v_L as a function of the state variables x_1, x_2 and the input u. Using Kirchhoff's voltage law, we can write an equation that the algebraic sum of all voltages across elements in the left loop is equal to zero:

$$v_C - E + Ri_L + v_L = 0$$

Hence,

$$v_L = -x_1 - Rx_2 + u$$

We can now write the state model for the circuit as

$$\dot{x}_1 = \frac{1}{C}\left[-h(x_1) + x_2\right] \tag{1.11}$$

$$\dot{x}_2 = \frac{1}{L}\left[-x_1 - Rx_2 + u\right] \tag{1.12}$$

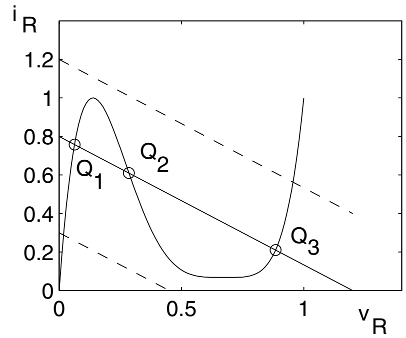

Figure 1.3: Equilibrium points of the tunnel-diode circuit.

The equilibrium points of the system are determined by setting $\dot{x}_1 = \dot{x}_2 = 0$ and solving for x_1 and x_2:

$$\begin{aligned} 0 &= -h(x_1) + x_2 \\ 0 &= -x_1 - Rx_2 + u \end{aligned}$$

Therefore, the equilibrium points correspond to the roots of the equation

$$h(x_1) = \frac{E}{R} - \frac{1}{R}x_1$$

Figure 1.3 shows graphically that, for certain values of E and R, this equation has three isolated roots which correspond to three isolated equilibrium points of the system. The number of equilibrium points might change as the values of E and R change. For example, if we increase E for the same value of R, we will reach a point beyond which only the point Q_3 will exist. On the other hand, if we decrease E for the same value of R, we will end up with the point Q_1 as the only equilibrium. Suppose that we are in the multiple equilibria situation, which of these equilibrium points can we observe in an experimental setup of this circuit? The answer depends on the stability properties of the equilibrium points. We will come back to this example in Chapter 2 and answer the question.

1.2.3 Mass–Spring System

In the mass–spring mechanical system, shown in Figure 1.4, we consider a mass m sliding on a horizontal surface and attached to a vertical surface through a spring. The mass is subjected to an external force F. We define y as the displacement from a reference position and write Newton's law of motion

$$m\ddot{y} + F_f + F_{sp} = F$$

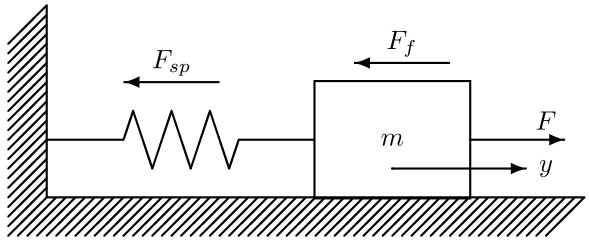

Figure 1.4: Mass-spring mechanical system.

where F_f is a resistive force due to friction and F_{sp} is the restoring force of the spring. We assume that F_{sp} is a function only of the displacement y and write it as $F_{sp} = g(y)$. We assume also that the reference position has been chosen such that $g(0) = 0$. The external force F is at our disposal. Depending upon F, F_f, and g, several interesting autonomous and nonautonomous second-order models arise.

For a relatively small displacement, the restoring force of the spring can be modeled as a linear function $g(y) = ky$, where k is the spring constant. For a large displacement, however, the restoring force may depend nonlinearly on y. For example, the function

$$g(y) = k(1 - a^2y^2)y, \quad |ay| < 1$$

models the so-called *softening spring*, where, beyond a certain displacement, a large displacement increment produces a small force increment. On the other hand, the function

$$g(y) = k(1 + a^2y^2)y$$

models the so-called *hardening spring*, where, beyond a certain displacement, a small displacement increment produces a large force increment.

The resistive force F_f may have components due to static, Coulomb, and viscous friction. When the mass is at rest, there is a static friction force F_s that acts parallel to the surface and is limited to $\pm\mu_s mg$, where $0 < \mu_s < 1$ is the static friction coefficient. This force takes whatever value, between its limits, to keep the mass at rest. For motion to begin, there must be a force acting on the mass to overcome the resistance to motion caused by static friction. In the absence of an external force, $F = 0$, the static friction force will balance the restoring force of the spring and maintain equilibrium for $|g(y)| \le \mu_s mg$. Once motion has started, the resistive force F_f, which acts in the direction opposite to motion, is modeled as a function of the sliding velocity $v = \dot{y}$. The resistive force due to *Coulomb friction* F_c has a constant magnitude $\mu_k mg$, where μ_k is the kinetic friction coefficient, that is,

$$F_c = \begin{cases} -\mu_k mg, & \text{for} \quad v < 0 \\ \mu_k mg, & \text{for} \quad v > 0 \end{cases}$$

As the mass moves in a viscous medium, such as air or lubricant, there will be a frictional force due to viscosity. This force is usually modeled as a nonlinear

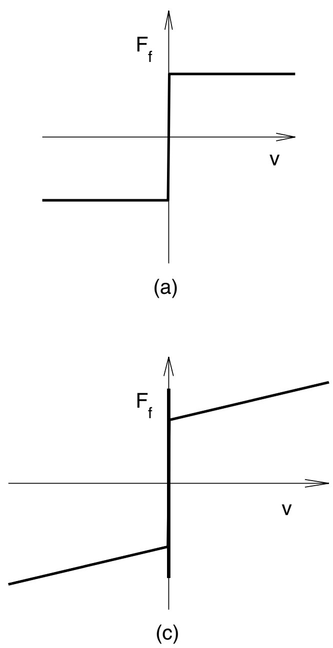

Figure 1.5: Examples of friction models. (a) Coulomb friction; (b) Coulomb plus linear viscous friction; (c) static, Coulomb, and linear viscous friction; (d) static, Coulomb, and linear viscous friction—Stribeck effect.

function of the velocity; that is, $F_v = h(v)$, where $h(0) = 0$. For small velocity, we can assume that $F_v = cv$. Figures 1.5(a) and (b) show examples of friction models for Coulomb friction and Coulombs plus linear viscous friction, respectively. Figure 1.5(c) shows an example where the static friction is higher than the level of Coulomb friction, while Figure 1.5(d) shows a similar situation, but with the force decreasing continuously with increasing velocity, the so-called *Stribeck effect*.

The combination of a hardening spring, linear viscous friction, and a periodic external force $F = A\cos\omega t$ results in the Duffing's equation

$$m\ddot{y} + c\dot{y} + ky + ka^2y^3 = A\cos\omega t \tag{1.13}$$

which is a classical example in the study of periodic excitation of nonlinear systems.

The combination of a linear spring, static friction, Coulomb friction, linear viscous friction, and zero external force results in

$$m\ddot{y} + ky + c\dot{y} + \eta(y, \dot{y}) = 0$$

where

$$\eta(y,\dot{y}) = \begin{cases} \mu_k mg \ \mathrm{sign}(\dot{y}), & \text{for} \quad |\dot{y}| > 0 \\ -ky, & \text{for} \quad \dot{y} = 0 \ \text{ and } \ |y| \le \mu_s mg/k \\ -\mu_s mg \ \mathrm{sign}(y), & \text{for} \quad \dot{y} = 0 \ \text{ and } \ |y| > \mu_s mg/k \end{cases}$$

The value of $\eta(y, \dot{y})$ for $\dot{y} = 0$ and $|y| \le \mu_s mg/k$ is obtained from the equilibrium condition $\ddot{y} = \dot{y} = 0$. With $x_1 = y$ and $x_2 = \dot{y}$, the state model is

$$\dot{x}_1 = x_2 \tag{1.14}$$

$$\dot{x}_2 = -\frac{k}{m}x_1 - \frac{c}{m}x_2 - \frac{1}{m}\eta(x_1, x_2) \tag{1.15}$$

Let us note two features of this state model. First, it has an equilibrium set, rather than isolated equilibrium points. Second, the right-hand side function is a discontinuous function of the state. The discontinuity is a consequence of the idealization we adopted in modeling friction. One would expect the physical friction to change from its static friction mode into its sliding friction mode in a smooth way, not abruptly as our idealization suggests.[3] The discontinuous idealization, however, simplifies the analysis. For example, when $x_2 > 0$, we can model the system by the linear model

$$\begin{aligned} \dot{x}_1 &= x_2 \\ \dot{x}_2 &= -\frac{k}{m}x_1 - \frac{c}{m}x_2 - \mu_k g \end{aligned}$$

Similarly, when $x_2 < 0$, we can model it by the linear model

$$\begin{aligned} \dot{x}_1 &= x_2 \\ \dot{x}_2 &= -\frac{k}{m}x_1 - \frac{c}{m}x_2 + \mu_k g \end{aligned}$$

Thus, in each region, we can predict the behavior of the system via linear analysis. This is an example of the so-called *piecewise linear analysis*, where a system is represented by linear models in various regions of the state space, certain coefficients changing from region to region.

1.2.4 Negative-Resistance Oscillator

Figure 1.6 shows the basic circuit structure of an important class of electronic oscillators. The inductor and capacitor are assumed to be linear, time invariant and passive, that is, $L > 0$ and $C > 0$. The resistive element is an active circuit characterized by the v–i characteristic $i = h(v)$, shown in the figure. The function

[3] The smooth transition from static to sliding friction can be captured by dynamic friction models; see, for example, [12] and [144].

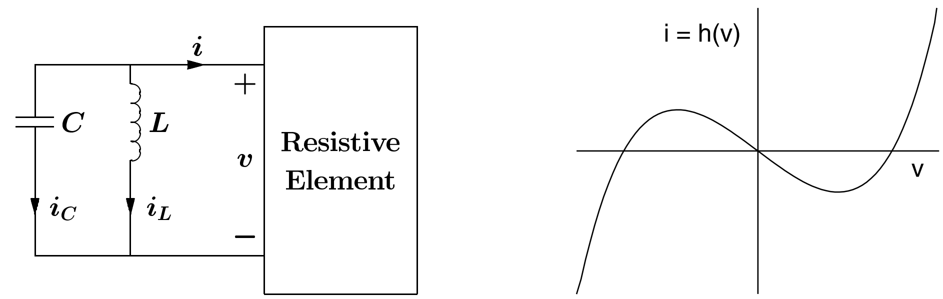

(a) (b)

Figure 1.6: (a) Basic oscillator circuit; (b) Typical driving-point characteristic.

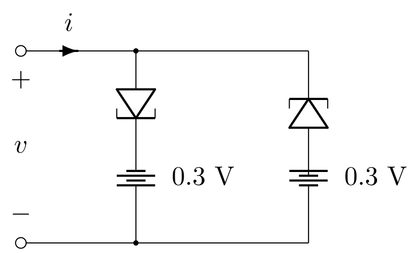

Figure 1.7: A negative-resistance twin-tunnel-diode circuit.

$h(\cdot)$ satisfies the conditions

$$h(0) = 0, \qquad h'(0) < 0$$

$$h(v) \to \infty \text{ as } v \to \infty, \quad \text{and} \quad h(v) \to -\infty \text{ as } v \to -\infty$$

where $h'(v)$ is the first derivative of $h(v)$ with respect to v. Such v–i characteristic can be realized, for example, by the twin-tunnel-diode circuit of Figure 1.7, with the tunnel-diode characteristic shown in Figure 1.2. Using Kirchhoff's current law, we can write the equation

$$i_C + i_L + i = 0$$

Hence,

$$C\frac{dv}{dt} + \frac{1}{L}\int_{-\infty}^{t} v(s)\ ds + h(v) = 0$$

Differentiating once with respect to t and multiplying through by L, we obtain

$$CL\frac{d^2v}{dt^2} + v + Lh'(v)\frac{dv}{dt} = 0$$

The foregoing equation can be written in a form that coincides with some well-known equations in nonlinear systems theory. To do that, let us change the time variable from t to $\tau = t/\sqrt{CL}$. The derivatives of v with respect to t and τ are related by

$$\frac{dv}{d\tau} = \sqrt{CL}\frac{dv}{dt} \quad \text{and} \quad \frac{d^2v}{d\tau^2} = CL\frac{d^2v}{dt^2}$$

Denoting the derivative of v with respect to τ by $\dot{v}$, we can rewrite the circuit equation as

$$\ddot{v} + \varepsilon h'(v)\dot{v} + v = 0$$

where $\varepsilon = \sqrt{L/C}$. This equation is a special case of *Liénard's equation*

$$\ddot{v} + f(v)\dot{v} + g(v) = 0 \tag{1.16}$$

When

$$h(v) = -v + \tfrac{1}{3}v^3$$

the circuit equation takes the form

$$\ddot{v} - \varepsilon(1 - v^2)\dot{v} + v = 0 \tag{1.17}$$

which is known as the *Van der Pol equation*. This equation, which was used by Van der Pol to study oscillations in vacuum tube circuits, is a fundamental example in nonlinear oscillation theory. It possesses a periodic solution that attracts every other solution except the zero solution at the unique equilibrium point $v = \dot{v} = 0$. To write a state model for the circuit, let us take $x_1 = v$ and $x_2 = \dot{v}$ to obtain

$$\dot{x}_1 = x_2 \tag{1.18}$$
$$\dot{x}_2 = -x_1 - \varepsilon h'(x_1)x_2 \tag{1.19}$$

Note that an alternate state model could have been obtained by choosing the state variables as the voltage across the capacitor and the current through the inductor. Denoting the state variables by $z_1 = i_L$ and $z_2 = v_C$, the state model is given by

$$\begin{aligned} \frac{dz_1}{dt} &= \frac{1}{L}z_2 \\ \frac{dz_2}{dt} &= -\frac{1}{C}[z_1 + h(z_2)] \end{aligned}$$

Since the first state model has been written with respect to the time variable $\tau = t/\sqrt{CL}$, let us write this model with respect to τ.

$$\dot{z}_1 = \frac{1}{\varepsilon}z_2 \tag{1.20}$$
$$\dot{z}_2 = -\varepsilon[z_1 + h(z_2)] \tag{1.21}$$

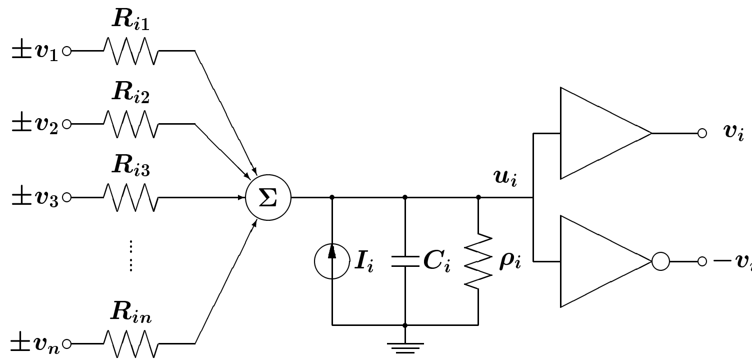

Figure 1.8: Hopfield neural network model.

The state models in x and z look different, but they are equivalent representations of the system. This equivalence can be seen by noting that these models can be obtained from each other by a change of coordinates

$$z = T(x)$$

Since we have chosen both x and z in terms of the physical variables of the circuit, it is not hard to find the map $T(\cdot)$. We have

$$\begin{aligned} x_1 &= v = z_2 \\ x_2 &= \frac{dv}{d\tau} = \sqrt{CL}\frac{dv}{dt} = \sqrt{\frac{L}{C}}[-i_L - h(v_C)] = \varepsilon[-z_1 - h(z_2)] \end{aligned}$$

Thus,

$$z = T(x) = \begin{bmatrix} -h(x_1) - (1/\varepsilon)x_2 \\ x_1 \end{bmatrix}$$

and the inverse mapping is

$$x = T^{-1}(z) = \begin{bmatrix} z_2 \\ -\varepsilon z_1 - \varepsilon h(z_2) \end{bmatrix}$$

1.2.5 Artificial Neural Network

Artificial neural networks, in analogy to biological structures, take advantage of distributed information processing and their inherent potential for parallel computation. Figure 1.8 shows an electric circuit that implements one model of neural networks, known as the *Hopfield model.* The circuit is based on an RC network con-

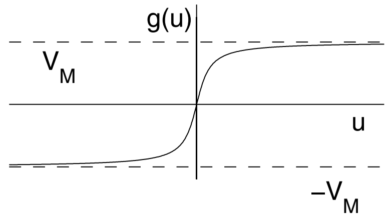

Figure 1.9: A typical input–output characteristic for the amplifiers in Hopfield network.

necting amplifiers. The input–output characteristics of the amplifiers are given by $v_i = g_i(u_i)$, where u_i and v_i are the input and output voltages of the ith amplifier. The function $g_i(\cdot) : R \to (-V_M, V_M)$ is a sigmoid function with asymptotes $-V_M$ and V_M, as shown in Figure 1.9. It is continuously differentiable, odd, monotonically increasing, and $g_i(u_i) = 0$ if and only if $u_i = 0$. Examples of possible $g_i(\cdot)$ are

$$g_i(u_i) = \frac{2V_M}{\pi} \tan^{-1}\left(\frac{\lambda \pi u_i}{2V_M}\right), \quad \lambda > 0$$

and

$$g_i(u_i) = V_M \frac{e^{\lambda u_i} - e^{-\lambda u_i}}{e^{\lambda u_i} + e^{-\lambda u_i}} = V_M \tanh(\lambda u_i), \quad \lambda > 0$$

where λ determines the slope of $g_i(u_i)$ at $u_i = 0$. Such sigmoid input–output characteristics can be realized by using operational amplifiers. For each amplifier, the circuit contains an inverting amplifier whose output is $-v_i$, which permits a choice of the sign of the amplifier output that is connected to a given input line. The outputs v_i and $-v_i$ are usually provided by two output terminals of the same operational amplifier circuit. The pair of nonlinear amplifiers is referred to as a "neuron." The circuit also contains an RC section at the input of each amplifier. The capacitance $C_i > 0$ and the resistance $\rho_i > 0$ represent the total shunt capacitance and shunt resistance at the ith amplifier input. Writing Kirchhoff's current law at the input node of the ith amplifier, we obtain

$$C_i \frac{du_i}{dt} = \sum_j \frac{1}{R_{ij}}(\pm v_j - u_i) - \frac{1}{\rho_i} u_i + I_i = \sum_j T_{ij} v_j - \frac{1}{R_i} u_i + I_i$$

where

$$\frac{1}{R_i} = \frac{1}{\rho_i} + \sum_j \frac{1}{R_{ij}}$$

T_{ij} is a signed conductance whose magnitude is $1/R_{ij}$, and whose sign is determined by the choice of the positive or negative output of the jth amplifier, and I_i is a constant input current. For a circuit containing n amplifiers, the motion is described by n first-order differential equations. To write a state model for the circuit, let us choose the state variables as $x_i = v_i$ for $i = 1, 2, \ldots, n$. Then

$$\dot{x}_i = \frac{dg_i}{du_i}(u_i) \times \dot{u}_i = \frac{dg_i}{du_i}(u_i) \times \frac{1}{C_i}\left(\sum_j T_{ij}x_j - \frac{1}{R_i}u_i + I_i\right)$$

By defining

$$h_i(x_i) = \left.\frac{dg_i}{du_i}(u_i)\right|_{u_i = g_i^{-1}(x_i)}$$

we can write the state equation as

$$\dot{x}_i = \frac{1}{C_i}h_i(x_i)\left[\sum_j T_{ij}x_j - \frac{1}{R_i}g_i^{-1}(x_i) + I_i\right] \tag{1.22}$$

for $i = 1, 2, \ldots, n$. Note that, due to the sigmoid characteristic of $g_i(\cdot)$, the function $h_i(\cdot)$ satisfies

$$h_i(x_i) > 0, \quad \forall\ x_i \in (-V_M, V_M)$$

The equilibrium points of the system are the roots of the n simultaneous equations

$$0 = \sum_j T_{ij}x_j - \frac{1}{R_i}g_i^{-1}(x_i) + I_i, \quad 1 \le i \le n$$

They are determined by the sigmoid characteristics, the linear resistive connection, and the input currents. We can obtain an equivalent state model by choosing the state variables as u_i for $i = 1, 2, \ldots, n$.

Stability analysis of this neural network depends critically on whether the symmetry condition $T_{ij} = T_{ji}$ is satisfied. An example of the analysis when $T_{ij} = T_{ji}$ is given in Section 4.2, while an example when $T_{ij} \neq T_{ji}$ is given in Section 9.5.

1.2.6 Adaptive Control

Consider a first-order linear system described by the model

$$\dot{y}_p = a_p y_p + k_p u$$

where u is the control input and y_p is the measured output. We refer to this system as the plant. Suppose that it is desirable to obtain a closed-loop system whose input–output behavior is described by the reference model

$$\dot{y}_m = a_m y_m + k_m r$$

where r is the reference input and the model has been chosen such that $y_m(t)$ represents the desired output of the closed-loop system. This goal can be achieved by the linear feedback control

$$u(t) = \theta_1^* r(t) + \theta_2^* y_p(t)$$

provided that the plant parameters a_p and k_p are known, $k_p \neq 0$, and the controller parameters θ_1^* and θ_2^* are chosen as

$$\theta_1^* = \frac{k_m}{k_p} \quad \text{and} \quad \theta_2^* = \frac{a_m - a_p}{k_p}$$

When a_p and k_p are unknown, we may consider the controller

$$u(t) = \theta_1(t)r(t) + \theta_2(t)y_p(t)$$

where the time-varying gains $\theta_1(t)$ and $\theta_2(t)$ are adjusted on-line by using the available data, namely, $r(\tau)$, $y_m(\tau)$, $y_p(\tau)$, and $u(\tau)$ for $\tau < t$. The adaptation should be such that $\theta_1(t)$ and $\theta_2(t)$ evolve to their nominal values θ_1^* and θ_2^*. The adaptation rule is chosen based on stability considerations. One such rule, known as the gradient algorithm,[4] is to use

$$\begin{aligned} \dot{\theta}_1 &= -\gamma(y_p - y_m)r \\ \dot{\theta}_2 &= -\gamma(y_p - y_m)y_p \end{aligned}$$

where γ is a positive constant that determines the speed of adaptation. This adaptive control law assumes that the sign of k_p is known and, without loss of generality, takes it to be positive. To write a state model that describes the closed-loop system under the adaptive control law, it is more convenient to define the output error e_o and the parameter errors ϕ_1 and ϕ_2 as

$$e_o = y_p - y_m, \quad \phi_1 = \theta_1 - \theta_1^*, \quad \text{and} \quad \phi_2 = \theta_2 - \theta_2^*$$

By using the definition of θ_1^* and θ_2^*, the reference model can be rewritten as

$$\dot{y}_m = a_p y_m + k_p(\theta_1^* r + \theta_2^* y_m)$$

On the other hand, the plant output y_p satisfies the equation

$$\dot{y}_p = a_p y_p + k_p(\theta_1 r + \theta_2 y_p)$$

Subtracting the above two equations, we obtain the error equation

$$\begin{aligned} \dot{e}_o &= a_p e_o + k_p(\theta_1 - \theta_1^*)r + k_p(\theta_2 y_p - \theta_2^* y_m) \\ &= a_p e_o + k_p(\theta_1 - \theta_1^*)r + k_p(\theta_2 y_p - \theta_2^* y_m + \theta_2^* y_p - \theta_2^* y_p) \\ &= (a_p + k_p\theta_2^*)e_o + k_p(\theta_1 - \theta_1^*)r + k_p(\theta_2 - \theta_2^*)y_p \end{aligned}$$

Thus, the closed-loop system is described by the nonlinear, nonautonomous, third-order state model

$$\dot{e}_o = a_m e_o + k_p\phi_1 r(t) + k_p\phi_2[e_o + y_m(t)] \tag{1.23}$$

$$\dot{\phi}_1 = -\gamma e_o r(t) \tag{1.24}$$

$$\dot{\phi}_2 = -\gamma e_o[e_o + y_m(t)] \tag{1.25}$$

[4]This adaptation rule will be justified in Section 8.3.

where we used $\dot{\phi}_i(t) = \dot{\theta}_i(t)$ and wrote $r(t)$ and $y_m(t)$ as explicit functions of time to emphasize the nonautonomous nature of the system. The signals $r(t)$ and $y_m(t)$ are the external driving inputs of the closed-loop system.

A simpler version of this model arises if we know k_p. In this case, we can take $\theta_1 = \theta_1^*$ and only θ_2 needs to be adjusted on-line. The closed-loop model reduces to

$$\dot{e}_o = a_m e_o + k_p \phi [e_o + y_m(t)] \tag{1.26}$$
$$\dot{\phi} = -\gamma e_o [e_o + y_m(t)] \tag{1.27}$$

where we dropped the subscript from ϕ_2. If the goal of the control design is to regulate the plant output y_p to zero, we take $r(t) \equiv 0$ (hence, $y_m(t) \equiv 0$) and the closed-loop model simplifies to the autonomous second-order model

$$\begin{aligned} \dot{e}_o &= (a_m + k_p \phi) e_o \\ \dot{\phi} &= -\gamma e_o^2 \end{aligned}$$

The equilibrium points of this system are determined by setting $\dot{e}_o = \dot{\phi} = 0$ to obtain the algebraic equations

$$\begin{aligned} 0 &= (a_m + k_p \phi) e_o \\ 0 &= -\gamma e_o^2 \end{aligned}$$

The system has equilibrium at $e_o = 0$ for all values of ϕ; that is, it has an equilibrium set $e_o = 0$. There are no isolated equilibrium points.

The particular adaptive control scheme described here is called *direct model reference adaptive control*. The term "model reference" stems from the fact that the controller's task is to match a given closed-loop reference model, while the term "direct" is used to indicate that the controller parameters are adapted directly as opposed, for example, to an adaptive control scheme that would estimate the plant parameters a_p and k_p on-line and use their estimates to calculate the controller parameters.[5] The adaptive control problem generates some interesting nonlinear models that will be used to illustrate some of the stability and perturbation techniques of this book.

1.2.7 Common Nonlinearities

In the foregoing examples, we saw some typical nonlinearities that arise in modeling physical systems, such as nonlinear resistance, nonlinear friction, and sigmoid nonlinearities. In this section, we cover some other typical nonlinearities. Figure 1.10 shows four typical memoryless nonlinearities. They are called memoryless, zero memory, or static because the output of the nonlinearity at any instant of time is

[5] For a comprehensive treatment of adaptive control, the reader may consult [5], [15], [87], [139], or [168].

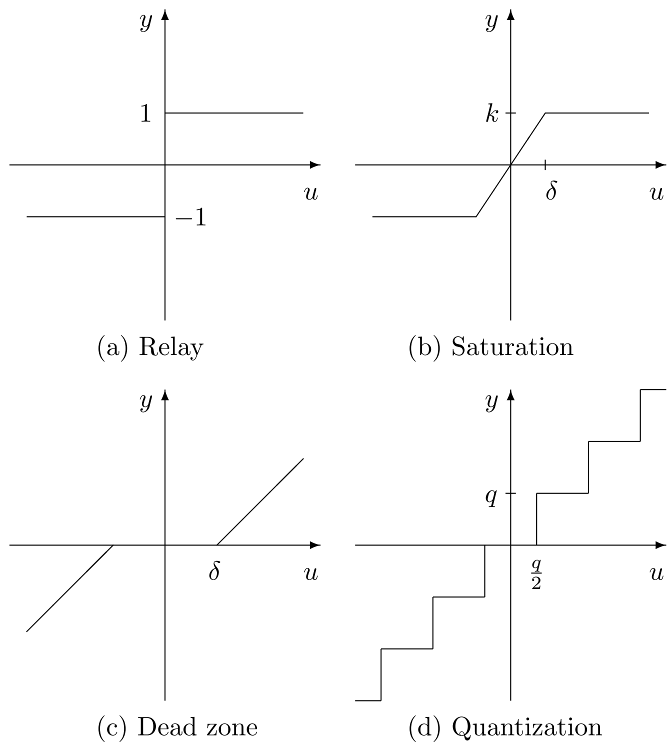

Figure 1.10: Typical memoryless nonlinearities.

determined uniquely by its input at that instant; it does not depend on the history of the input.

Figure 1.10(a) shows an ideal relay described by the signum function

$$\mathrm{sgn}(u) = \begin{cases} 1, & \text{if } u > 0 \\ 0, & \text{if } u = 0 \\ -1, & \text{if } u < 0 \end{cases} \tag{1.28}$$

Such nonlinear characteristic can model electromechanical relays, thyristor circuits, and other switching devices.

Figure 1.10(b) shows an ideal saturation nonlinearity. Saturation characteristics are common in all practical amplifiers (electronic, magnetic, pneumatic, or hydraulic), motors, and other devices. They are also used, intentionally, as limiters to restrict the range of a variable. We define the saturation function

$$\mathrm{sat}(u) = \begin{cases} u, & \text{if } |u| \le 1 \\ \mathrm{sgn}(u), & \text{if } |u| > 1 \end{cases} \tag{1.29}$$

to represent a normalized saturation nonlinearity and generate the graph of Fig-

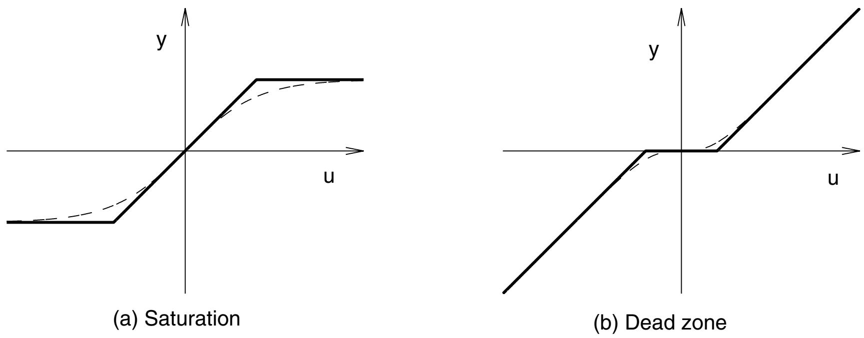

Figure 1.11: Practical characteristics (dashed) of saturation and dead-zone nonlinearities are approximated by piecewise linear characteristics (solid).

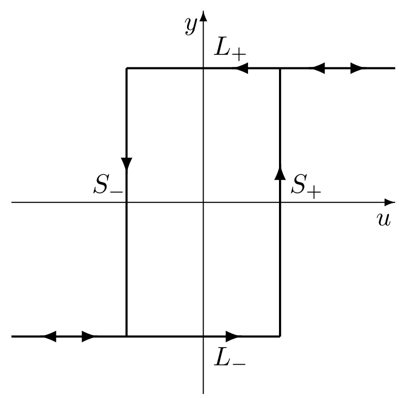

Figure 1.12: Relay with hysteresis.

ure 1.10(b) as k sat(u/δ).

Figure 1.10(c) shows an ideal dead-zone nonlinearity. Such characteristic is typical of valves and some amplifiers at low input signals. The piecewise linear functions used in Figure 1.10(b) and (c) to represent saturation and dead-zone characteristics are approximations of more realistic smooth functions, as shown in Figure 1.11

Figure 1.10(d) shows a quantization nonlinearity, which is typical in analog-to-digital conversion of signals.

Quite frequently, we encounter nonlinear elements whose input–output characteristics have memory; that is, the output at any instant of time may depend on the whole history of the input. Figures 1.12, 1.15(b), and 1.16 show three such characteristics of the hysteresis type. The first of the three elements, Figure 1.12, is a relay with hysteresis. For highly negative values of the input, the output will

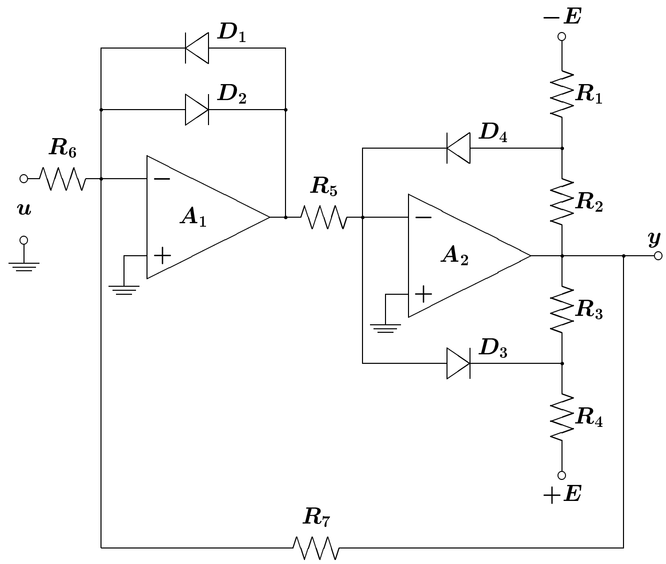

Figure 1.13: An operational amplifier circuit that realizes the relay with hysteresis characteristic of Figure 1.12.

be at the lower level L_-. As the input is increased, the output stays at L_- until the input reaches S_+. Increasing the input beyond S_+, the output switches to the higher level L_+ and stays there for higher values of the input. Now, if we decrease the input, the output stays at the higher level L_+ until the input crosses the value S_- at which point the output switches to the lower level L_- and stays there for lower values of the input. Such input–output characteristic can be generated, for example, by the operational amplifier circuit of Figure 1.13.[6] The circuit features ideal operational amplifiers and ideal diodes. An ideal operational amplifier has the voltage at its inverting (-) input equal to the voltage at its noninverting (+) input and has zero input currents at both inputs. An ideal diode has the v–i characteristic shown in Figure 1.14. When the input voltage u is highly negative, the diodes D_1 and D_3 will be *on* while D_2 and D_4 will be *off*.[7] Because the inverting inputs of both amplifiers are at virtual ground, the currents in R_5 and D_3 will be zero and the output of D_3 will be at virtual ground. Therefore, the output voltage y will be given by $y = -(R_3/R_4)E$. This situation will remain as long as the current in D_1

[6] This circuit is taken from [204].

[7] To see why D_3 is *on* when D_1 is *on*, notice that when D_1 is *on*, the voltage at the output of A_1 will be V_d, the offset voltage of the diode. This will cause a current V_d/R_5 to flow in R_5 heading towards A_2. Since the input current to A_2 is zero, the current in R_5 must flow through D_3. In modeling the diodes, we neglect the offset voltage V_d; therefore, the currents in R_5 and D_3 are neglected.

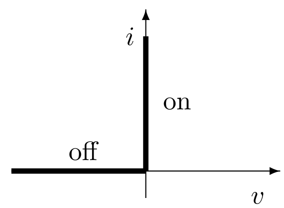

Figure 1.14: v–i characteristic of an ideal diode.

is positive; that is,

$$i_{D1} = \frac{R_3 E}{R_4 R_7} - \frac{u}{R_6} > 0 \;\Leftrightarrow\; u < \frac{R_3 R_6 E}{R_4 R_7}$$

As we increase the input u, the output y will stay at $-(R_3/R_4)E$ until the input reaches the value R_3R_6E/R_4R_7. Beyond this value, the diodes D_1 and D_3 will be *off* while D_2 and D_4 will be *on*. Once again, because the inverting inputs of both amplifiers are at virtual ground, the currents in R_5 and D_4 will be zero, and the input of D_4 will be at virtual ground. Therefore, the output y will be given by $y = (R_2/R_1)E$. This situation will remain as long as the current in D_2 is positive; that is,

$$i_{D2} = \frac{u}{R_6} + \frac{R_2 E}{R_1 R_7} > 0 \;\Leftrightarrow\; u > -\frac{R_2 R_6 E}{R_1 R_7}$$

Thus, we obtain the input–output characteristic of Figure 1.12 with

$$L_- = -\frac{R_3 E}{R_4}, \quad L_+ = \frac{R_2 E}{R_1}, \quad S_- = -\frac{R_2 R_6 E}{R_1 R_7}, \quad S_+ = \frac{R_3 R_6 E}{R_4 R_7}$$

We will see in Example 2.1 that the tunnel-diode circuit of Section 1.2.2 produces a similar characteristic when its input voltage is much slower than the dynamics of the circuit.

Another type of hysteresis nonlinearity is the backlash characteristic shown in Figure 1.15(b), which is common in gears. To illustrate backlash, the sketch of Figure 1.15(a) shows a small gap between a pair of mating gears. Suppose that the driven gear has a high friction to inertia ratio so that when the driving gear starts to decelerate, the surfaces will remain in contact at L. The input–output characteristic shown in Figure 1.15(b) depicts the angle of the driven gear y versus the angle of the driving gear u. Starting from the position shown in Figure 1.15(a), when the driving gear rotates an angle smaller than a, the driven gear does not move. For rotation larger than a, a contact is established at L and the driven gear follows the driving one, corresponding to the A_oA piece of the input–output characteristic. When the driving gear reverses direction, it rotates an angle $2a$ before a contact is established at U. During this motion, the angle y remains constant, producing the AB piece of

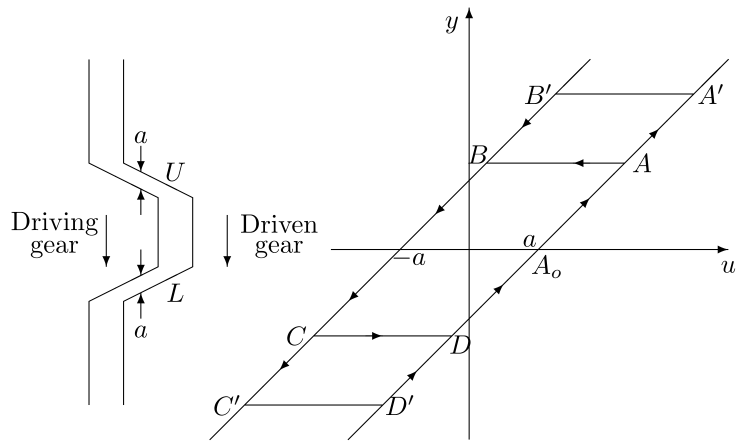

(a) (b)

Figure 1.15: Backlash nonlinearity.

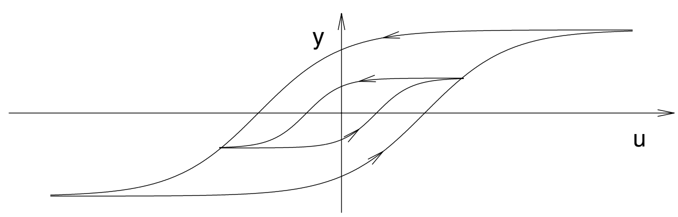

Figure 1.16: Hysteresis nonlinearity.

the characteristic. After a contact is established at U, the driven gear follows the driving one, producing the BC piece, until another reversal of direction produces the CDA piece. Thus, a periodic input of amplitude higher than a produces the $ABCD$ hysteresis loop of Figure 1.15(b). Notice that for a larger amplitude, the hysteresis loop will be $A'B'C'D'$—an important difference between this type of hysteresis characteristic and the relay with hysteresis characteristic of Figure 1.12, where the hysteresis loop is independent of the amplitude of the input.

Similar to backlash, the hysteresis characteristic of Figure 1.16, which is typical in magnetic material, has a hysteresis loop that is dependent on the amplitude of the input.[8]

[8]Modeling the hysteresis characteristics of Figures 1.15(b) and 1.16 is quite complex. Various modeling approaches are given in [106], [126] and [203].

1.3 Exercises

1.1 A mathematical model that describes a wide variety of physical nonlinear systems is the nth-order differential equation

$$y^{(n)} = g\left(t, y, \dot{y}, \ldots, y^{(n-1)}, u\right)$$

where u and y are scalar variables. With u as input and y as output, find a state model.

1.2 Consider a single-input–single-output system described by the nth-order differential equation

$$y^{(n)} = g_1\left(t, y, \dot{y}, \ldots, y^{(n-1)}, u\right) + g_2\left(t, y, \dot{y}, \ldots, y^{(n-2)}\right)\dot{u}$$

where g_2 is a differentiable function of its arguments. With u as input and y as output, find a state model.
Hint: Take $x_n = y^{(n-1)} - g_2\left(t, y, \dot{y}, \ldots, y^{(n-2)}\right)u$.

1.3 Consider a single-input–single-output system described by the nth-order differential equation

$$y^{(n)} = g\left(y, \ldots, y^{(n-1)}, z, \ldots, z^{(m)}\right), \quad m < n$$

where z is the input and y is the output. Extend the dynamics of the system by adding a series of m integrators at the input side and define $u = z^{(m)}$ as the input to the extended system; see Figure 1.17. Using $y, \ldots, y^{(n-1)}$ and $z, \ldots, z^{(m-1)}$ as state variables, find a state model of the extended system.

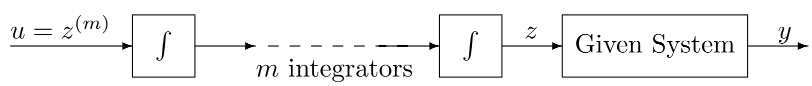

Figure 1.17: Exercise 1.3.

1.4 The nonlinear dynamic equations for an m-link robot [171, 185] take the form

$$M(q)\ddot{q} + C(q, \dot{q})\dot{q} + +D\dot{q} + g(q) = u$$

where q is an m-dimensional vector of generalized coordinates representing joint positions, u is an m-dimensional control (torque) input, and $M(q)$ is a symmetric inertia matrix, which is positive definite for all $q \in R^m$. The term $C(q, \dot{q})\dot{q}$ accounts for centrifugal and Coriolis forces. The matrix C has the property that $\dot{M} - 2C$ is a skew-symmetric matrix for all $q, \dot{q} \in R^m$, where $\dot{M}$ is the total derivative of $M(q)$ with respect to t. The term $D\dot{q}$ account for viscous damping, where D is a positive semidefinite symmetric matrix. The term $g(q)$, which accounts for gravity forces, is given by $g(q) = [\partial P(q)/\partial q]^T$, where $P(q)$ is the total potential energy of the links due to gravity. Choose appropriate state variables and find the state equation.

1.5 The nonlinear dynamic equations for a single-link manipulator with flexible joints [185], damping ignored, is given by

$$\begin{aligned} I\ddot{q}_1 + MgL\sin q_1 + k(q_1 - q_2) &= 0 \\ J\ddot{q}_2 - k(q_1 - q_2) &= u \end{aligned}$$

where q_1 and q_2 are angular positions, I and J are moments of inertia, k is a spring constant, M is the total mass, L is a distance, and u is a torque input. Choose state variables for this system and write down the state equation.

1.6 The nonlinear dynamic equations for an m-link robot with flexible joints [185] take the form

$$\begin{aligned} M(q_1)\ddot{q}_1 + h(q_1, \dot{q}_1) + K(q_1 - q_2) &= 0 \\ J\ddot{q}_2 - K(q_1 - q_2) &= u \end{aligned}$$

where q_1 and q_2 are m-dimensional vectors of generalized coordinates, $M(q_1)$ and J are symmetric nonsingular inertia matrices, and u is an m-dimensional control input. The term $h(q, \dot{q})$ accounts for centrifugal, Coriolis, and gravity forces, and K is a diagonal matrix of joint spring constants. Choose state variables for this system and write down the state equation.

1.7 Figure 1.18 shows a feedback connection of a linear time-invariant system represented by the transfer function $G(s)$ and a nonlinear time-varying element defined by $z = \psi(t, y)$. The variables r, u, y, and z are vectors of the same dimension, and $\psi(t, y)$ is a vector-valued function. With r as input and y as output, find a state model.

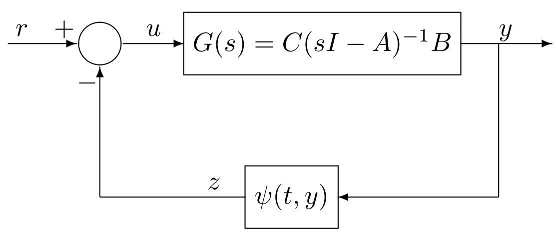

Figure 1.18: Exercise 1.7.

1.8 A synchronous generator connected to an infinite bus can be represented [148] by

$$\begin{aligned} M\ddot{\delta} &= P - D\dot{\delta} - \eta_1 E_q \sin\delta \\ \tau\dot{E}_q &= -\eta_2 E_q + \eta_3 \cos\delta + E_{FD} \end{aligned}$$

where δ is an angle in radians, E_q is voltage, P is mechanical input power, E_{FD} is field voltage (input), D is damping coefficient, M is inertial coefficient, τ is time constant, and η_1, η_2, and η_3 are constant parameters.

(a) Using δ, $\dot{\delta}$, and E_q as state variables, find the state equation.

(b) Let $P = 0.815$, $E_{FD} = 1.22$, $\eta_1 = 2.0$, $\eta_2 = 2.7$, $\eta_3 = 1.7$, $\tau = 6.6$, $M = 0.0147$, and $D/M = 4$. Find all equilibrium points.

(c) Suppose that τ is relatively large so that $\dot{E}_q \approx 0$. Show that assuming E_q to be constant reduces the model to a pendulum equation.

1.9 The circuit shown in Figure 1.19 contains a nonlinear inductor and is driven by a time-dependent current source. Suppose that the nonlinear inductor is a Josephson junction [39], described by $i_L = I_0 \sin k\phi_L$, where ϕ_L is the magnetic flux of the inductor and I_0 and k are constants.

(a) Using ϕ_L and v_C as state variables, find the state equation.

(b) Is it easier to choose i_L and v_C as state variables?

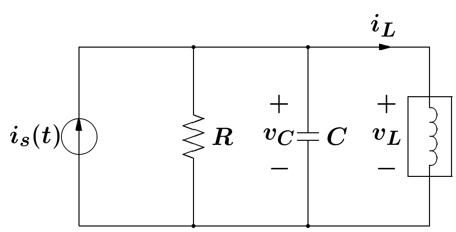

Figure 1.19: Exercises 1.9 and 1.10.

1.10 The circuit shown in Figure 1.19 contains a nonlinear inductor and is driven by a time-dependent current source. Suppose that the nonlinear inductor is described by $i_L = L\phi_L + \mu\phi_L^3$, where ϕ_L is the magnetic flux of the inductor and L and μ are positive constants.

(a) Using ϕ_L and v_C as state variables, find the state equation.

(b) Find all equilibrium points when $i_s = 0$.

1.11 A phase-locked loop [64] can be represented by the block diagram of Figure 1.20. Let $\{A, B, C\}$ be a minimal realization of the scalar, strictly proper transfer function $G(s)$. Assume that all eigenvalues of A have negative real parts, $G(0) \neq 0$, and $\theta_i =$ constant. Let z be the state of the realization $\{A, B, C\}$.

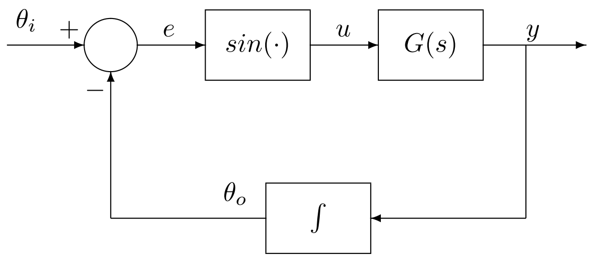

Figure 1.20: Exercise 1.11.

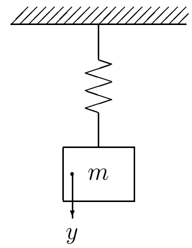

Figure 1.21: Exercise 1.12.

(a) Show that the closed-loop system can be represented by the state equations

$$\dot{z} = Az + B \sin e, \qquad \dot{e} = -Cz$$

(b) Find all equilibrium points of the system.

(c) Show that when $G(s) = 1/(\tau s + 1)$, the closed-loop model coincides with the model of a pendulum equation.

1.12 Consider the mass–spring system shown in Figure 1.21. Assuming a linear spring and nonlinear viscous damping described by $c_1\dot{y}+c_2\dot{y}|\dot{y}|$, find a state equation that describes the motion of the system.

1.13 An example of a mechanical system in which friction can be negative in a certain region is the structure shown in Figure 1.22 [7]. On a belt moving uniformly with velocity v_0, there lies a mass m fixed by linear springs, with spring constants k_1 and k_2. The friction force $h(v)$ exerted by the belt on the mass is a function of the relative velocity $v = v_0 - \dot{y}$. We assume that $h(v)$ is a smooth function for $|v| > 0$. In addition to this friction, assume that there is a linear viscous friction proportional to $\dot{y}$.

(a) Write down the equation of motion of the mass m.

(b) By restricting our analysis to the region $|\dot{y}| \ll v_0$, we can use a Taylor series to approximate $h(v)$ by $h(v_0) - \dot{y}h'(v_0)$. Using this approximation, simplify the model of the system.

(c) In view of the friction models discussed in Section 1.3, describe what kind of friction characteristic $h(v)$ would result in a system with negative friction.

1.14 Figure 1.23 shows a vehicle moving on a road with grade angle θ, where v the vehicle's velocity, M is its mass, and F is the tractive force generated by the engine. Assume that the friction is due to Coulomb friction, linear viscous friction, and a drag force proportional to v^2. Viewing F as the control input and θ as a disturbance input, find a state model of the system.

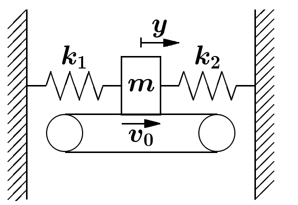

Figure 1.22: Exercise 1.13.

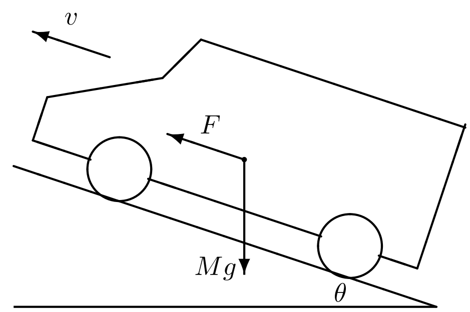

Figure 1.23: Exercise 1.14.

1.15 Consider the inverted pendulum of Figure 1.24 [110]. The pivot of the pendulum is mounted on a cart that can move in a horizontal direction. The cart is driven by a motor that exerts a horizontal force F on the cart. The figure shows also the forces acting on the pendulum, which are the force mg at the center of gravity, a horizontal reaction force H, and a vertical reaction force V at the pivot. Writing horizontal and vertical Newton's laws at the center of gravity of the pendulum yields

$$m\,\frac{d^2}{dt^2}(y + L\sin\theta) = H \quad \text{and} \quad m\,\frac{d^2}{dt^2}(L\cos\theta) = V - mg$$

Taking moments about the center of gravity yields the torque equation

$$I\ddot{\theta} = VL\sin\theta - HL\cos\theta$$

while a horizontal Newton's law for the cart yields

$$M\ddot{y} = F - H - k\dot{y}$$

Here m is the mass of the pendulum, M is the mass of the cart, L is the distance from the center of gravity to the pivot, I is the moment of inertia of the pendulum with respect to the center of gravity, k is a friction coefficient, y is the displacement of the pivot, θ is the angular rotation of the pendulum (measured clockwise), and g is the acceleration due to gravity.

(a) Carrying out the indicated differentiation and eliminating V and H, show that the equations of motion reduce to

$$I\ddot{\theta} = mgL\sin\theta - mL^2\ddot{\theta} - mL\ddot{y}\cos\theta$$

$$M\ddot{y} = F - m\left(\ddot{y} + L\ddot{\theta}\cos\theta - L\dot{\theta}^2\sin\theta\right) - k\dot{y}$$

(b) Solving the foregoing equations for $\ddot{\theta}$ and $\ddot{y}$, show that

$$\begin{bmatrix} \ddot{\theta} \\ \ddot{y} \end{bmatrix} = \frac{1}{\Delta(\theta)} \begin{bmatrix} m + M & -mL\cos\theta \\ -mL\cos\theta & I + mL^2 \end{bmatrix} \begin{bmatrix} mgL\sin\theta \\ F + mL\dot{\theta}^2\sin\theta - k\dot{y} \end{bmatrix}$$

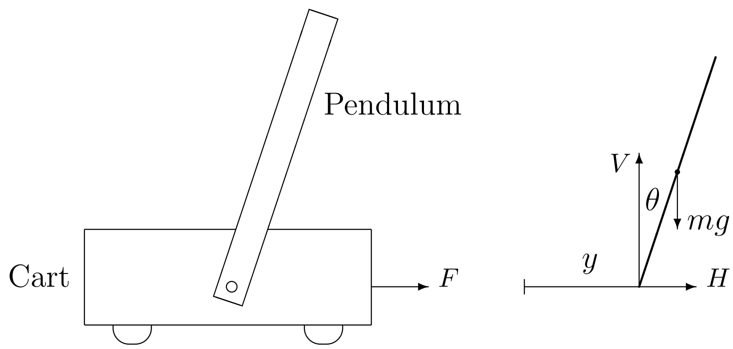

Figure 1.24: Inverted pendulum of Exercise 1.15.

where

$$\Delta(\theta) = (I + mL^2)(m + M) - m^2L^2\cos^2\theta \geq (I + mL^2)M + mI > 0$$

(c) Using $x_1 = \theta$, $x_2 = \dot{\theta}$, $x_3 = y$, and $x_4 = \dot{y}$ as the state variables and $u = F$ as the control input, write down the state equation.

1.16 Figure 1.25 shows a schematic diagram of a Translational Oscillator with Rotating Actuator (TORA) system [205]. The system consists of a platform of mass M connected to a fixed frame of reference by a linear spring, with spring constant k. The platform can only move in the horizontal plane, parallel to the spring axis. On the platform, a rotating proof mass is actuated by a DC motor. It has mass m and moment of inertial I around its center of mass, located at a distance L from its rotational axis. The control torque applied to the proof mass is denoted by u. The rotating proof mass creates a force which can be controlled to dampen the translational motion of the platform. We will derive a model for the system, neglecting friction. Figure 1.25 shows that the proof mass is subject to forces F_x and F_y and a torque u. Writing Newton's law at the center of mass and taking moments about the center of mass yield the equations

$$m\,\frac{d^2}{dt^2}(x_c + L\sin\theta) = F_x, \;\; m\,\frac{d^2}{dt^2}(L\cos\theta) = F_y, \;\; \text{and} \;\; I\ddot{\theta} = u + F_yL\sin\theta - F_xL\cos\theta$$

where θ is the angular position of the proof mass (measured counter clockwise). The platform is subject to the forces F_x and F_y, in the opposite directions, as well as the restoring force of the spring. Newton's law for the platform yields

$$M\ddot{x}_c = -F_x - kx_c$$

where x_c is the translational position of the platform.

(a) Carrying out the indicated differentiation and eliminating F_x and F_y, show that the equations of motion reduce to

$$D(\theta)\begin{bmatrix} \ddot{\theta} \\ \ddot{x}_c \end{bmatrix} = \begin{bmatrix} u \\ mL\dot{\theta}^2 \sin\theta - kx_c \end{bmatrix}, \text{ where } D(\theta) = \begin{bmatrix} I + mL^2 & mL\cos\theta \\ mL\cos\theta & M + m \end{bmatrix}$$

(b) Solving the foregoing equation for $\ddot{\theta}$ and $\ddot{x}_c$, show that

$$\begin{bmatrix} \ddot{\theta} \\ \ddot{x}_c \end{bmatrix} = \frac{1}{\Delta(\theta)}\begin{bmatrix} m + M & -mL\cos\theta \\ -mL\cos\theta & I + mL^2 \end{bmatrix}\begin{bmatrix} u \\ mL\dot{\theta}^2 \sin\theta - kx_c \end{bmatrix}$$

where

$$\Delta(\theta) = (I + mL^2)(m + M) - m^2L^2\cos^2\theta \geq (I + mL^2)M + mI > 0$$

(c) Using $x_1 = \theta$, $x_2 = \dot{\theta}$, $x_3 = x_c$, and $x_4 = \dot{x}_c$ as the state variables and u as the control input, write down the state equation.

(d) Find all equilibrium points of the system.

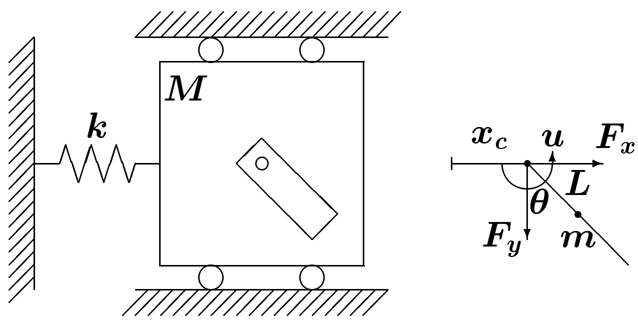

Figure 1.25: Translational Oscillator with Rotating Actuator (TORA) system.

1.17 The dynamics of a DC motor [178] can be described by

$$\begin{aligned} v_f &= R_f i_f + L_f \frac{di_f}{dt} \\ v_a &= c_1 i_f \omega + L_a \frac{di_a}{dt} + R_a i_a \\ J\frac{d\omega}{dt} &= c_2 i_f i_a - c_3 \omega \end{aligned}$$

The first equation is for the field circuit with v_f, i_f, R_f, and L_f being its voltage, current, resistance, and inductance. The variables v_a, i_a, R_a, and L_a are the corresponding variables for the armature circuit described by the second equation. The third equation is a torque equation for the shaft, with J as the rotor inertia and c_3 as a damping coefficient. The term $c_1 i_f \omega$ is the back e.m.f. induced in the armature circuit, and $c_2 i_f i_a$ is the torque produced by the interaction of the armature current with the field circuit flux.

(a) For a separately excited DC motor, the voltages v_a and v_f are independent control inputs. Choose appropriate state variables and find the state equation.

(b) Specialize the state equation of part(a) to the field controlled DC motor, where v_f is the control input, while v_a is held constant.

(c) Specialize the state equation of part(a) to the armature controlled DC motor, where v_a is the control input, while v_f is held constant. Can you reduce the order of the model in this case?

(d) In a shunt wound DC motor, the field and armature windings are connected in parallel and an external resistance R_x is connected in series with the field winding to limit the field flux; that is, $v = v_a = v_f + R_x i_f$. With v as the control input, write down the state equation.

1.18 Figure 1.26 shows a schematic diagram of a magnetic suspension system, where a ball of magnetic material is suspended by means of an electromagnet whose current is controlled by feedback from the, optically measured, ball position [211, pp. 192–200]. This system has the basic ingredients of systems constructed to levitate mass, used in gyroscopes, accelerometers, and fast trains. The equation of motion of the ball is

$$m\ddot{y} = -k\dot{y} + mg + F(y, i)$$

where m is the mass of the ball, $y \geq 0$ is the vertical (downward) position of the ball measured from a reference point ($y = 0$ when the ball is next to the coil), k is a viscous friction coefficient, g is the acceleration due to gravity, $F(y, i)$ is the force generated by the electromagnet, and i is its electric current. The inductance of the electromagnet depends on the position of the ball and can be modeled as

$$L(y) = L_1 + \frac{L_0}{1 + y/a}$$

where L_1, L_0, and a are positive constants. This model represents the case that the inductance has its highest value when the ball is next to the coil and decreases to a constant value as the ball is removed to $y = \infty$. With $E(y, i) = \frac{1}{2}L(y)i^2$ as the energy stored in the electromagnet, the force $F(y, i)$ is given by

$$F(y, i) = \frac{\partial E}{\partial y} = -\frac{L_0 i^2}{2a(1 + y/a)^2}$$

When the electric circuit of the coil is driven by a voltage source with voltage v, Kirchhoff's voltage law gives the relationship $v = \dot{\phi} + Ri$, where R is the series resistance of the circuit and $\phi = L(y)i$ is the magnetic flux linkage.

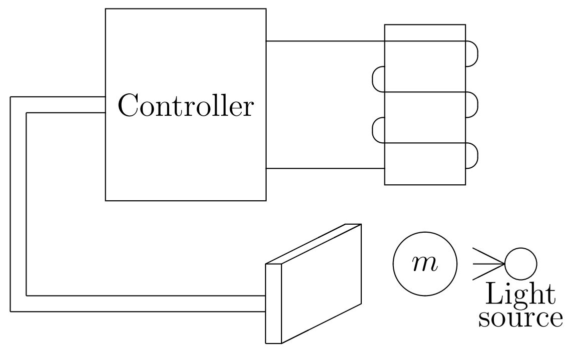

Figure 1.26: Magnetic suspension system of Exercise 1.18.

(a) Using $x_1 = y$, $x_2 = \dot{y}$, and $x_3 = i$ as state variables and $u = v$ as control input, find the state equation.

(b) Suppose it is desired to balance the ball at a certain position $r > 0$. Find the steady-state values I_{ss} and V_{ss} of i and v, respectively, which are necessary to maintain such balance.

The next three exercises give examples of hydraulic systems [41].

1.19 Figure 1.27 shows a hydraulic system where liquid is stored in an open tank. The cross-sectional area of the tank, $A(h)$, is a function of h, the height of the liquid level above the bottom of the tank. The liquid volume v is given by $v = \int_0^h A(\lambda)\, d\lambda$. For a liquid of density ρ, the absolute pressure p is given by $p = \rho g h + p_a$, where p_a is the atmospheric pressure (assumed constant) and g is the acceleration due to gravity. The tank receives liquid at a flow rate w_i and loses liquid through a valve that obeys the flow-pressure relationship $w_o = k\sqrt{\Delta p}$. In the current case, $\Delta p = p - p_a$. Take $u = w_i$ to be the control input and $y = h$ to be the output.

(a) Using h as the state variable, determine the state model.

(b) Using $p - p_a$ as the state variable, determine the state model.

(c) Find u_{ss} that is needed to maintain the output at a constant value r.

1.20 The hydraulic system shown in Figure 1.28 consists of a constant speed centrifugal pump feeding a tank from which liquid flows through a pipe and a valve that obeys the relationship $w_o = k\sqrt{p - p_a}$. The pump characteristic for the specified pump speed is shown in Figure 1.29. Let us denote this relationship by $\Delta p = \phi(w_i)$ and denote its inverse, whenever defined, by $w_i = \phi^{-1}(\Delta p)$. For the current pump, $\Delta p = p - p_a$. The cross-sectional area of the tank is uniform; therefore, $v = Ah$ and $p = p_a + \rho g v / A$, where the variables are defined in the previous exercise.

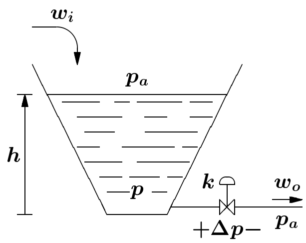

Figure 1.27: Exercise 1.19.

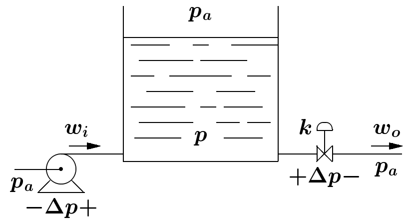

Figure 1.28: Exercise 1.20.

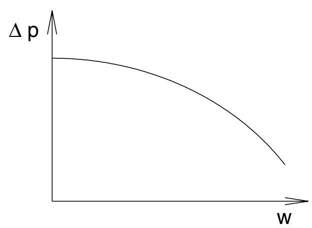

Figure 1.29: Typical centrifugal pump characteristic.

(a) Using $(p - p_a)$ as the state variable, find the state model.

(b) Find all equilibrium points of the system.

1.21 The valves in the hydraulic system of Figure 1.30 obey the flow relationships $w_1 = k_1\sqrt{p_1 - p_2}$ and $w_2 = k_2\sqrt{p_2 - p_a}$. The pump has the characteristic shown in Figure 1.29 for $(p_1 - p_a)$ versus w_p. The various components and variables are defined in the previous two exercises.

(a) Using $(p_1 - p_a)$ and $(p_2 - p_a)$ as the state variables, find the state equation.

(b) Find all equilibrium points of the system.

1.22 Consider a biochemical reactor with two components—biomass and substrate—where the biomass cells consume the substrate [23]; a schematic is shown in Figure 1.31. Assume that the reactor is perfectly mixed and the volume V is constant. Let x_1 and x_2 be the concentrations (mass/volume) of the biomass cells and substrate, respectively, and x_{1f} and x_{2f} be the corresponding concentrations in the feed stream. Let r_1 be the rate of biomass cell generation (mass/volume/time), r_2 be the rate of the substrate consumption, and F be the flow rate (volume/time). The dynamic model is developed by writing material balances on the biomass and substrate; that is,

$$\text{rate of biomass accumulation} = \text{in by flow} - \text{out by flow} + \text{generation}$$

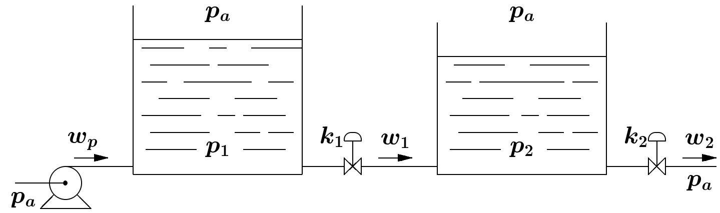

Figure 1.30: The hydraulic system of Exercise 1.21.

$$\text{rate of substrate accumulation} = \text{in by flow} - \text{out by flow} - \text{consumption}$$

The generation rate r_1 is modeled as $r_1 = \mu x_1$, where the specific growth coefficient μ is a function of x_2. We assume that there is no biomass in the feed stream, so $x_{1f} = 0$, the dilution rate $d = F/V$ is constant, and the yield $Y = r_1/r_2$ is constant.

(a) Using x_1 and x_2 as state variables, find the state model.

(b) Find all equilibrium points when $\mu = \mu_m x_2/(k_m + x_2)$ for some positive constants μ_m and k_m. Assume that $d < \mu_m$.

(c) Find all equilibrium points when $\mu = \mu_m x_2/(k_m + x_2 + k_1 x_2^2)$ for some positive constants μ_m, k_m, and k_1. Assume that $d < \max_{x_2 \geq 0}\{\mu(x_2)\}$.

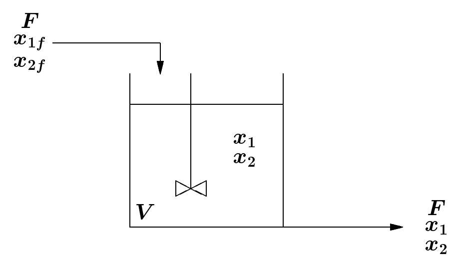

Figure 1.31: Biochemical reactor of Exercise 1.22.

Chapter 2

Second-Order Systems

Second-order autonomous systems occupy an important place in the study of nonlinear systems because solution trajectories can be represented by curves in the plane. This allows for easy visualization of the qualitative behavior of the system. The purpose of this chapter is to use second-order systems to introduce, in an elementary context, some of the basic ideas of nonlinear systems. In particular, we will look at the behavior of a nonlinear system near equilibrium points, the phenomenon of nonlinear oscillation, and bifurcation.

A second-order autonomous system is represented by two scalar differential equations

$$\dot{x}_1 = f_1(x_1, x_2) \tag{2.1}$$

$$\dot{x}_2 = f_2(x_1, x_2) \tag{2.2}$$

Let $x(t) = (x_1(t), x_2(t))$ be the solution[1] of (2.1)–(2.2) that starts at a certain initial state $x_0 = (x_{10}, x_{20})$; that is, $x(0) = x_0$. The locus in the x_1–x_2 plane of the solution $x(t)$ for all $t \geq 0$ is a curve that passes through the point x_0. This curve is called a *trajectory* or *orbit* of (2.1)–(2.2) from x_0. The x_1–x_2 plane is usually called the *state plane* or *phase plane*. The right-hand side of (2.1)–(2.2) expresses the tangent vector $\dot{x}(t) = (\dot{x}_1(t), \dot{x}_2(t))$ to the curve. Using the vector notation

$$\dot{x} = f(x)$$

where $f(x)$ is the vector $(f_1(x), f_2(x))$, we consider $f(x)$ as a *vector field* on the state plane, which means that to each point x in the plane, we assign a vector $f(x)$. For easy visualization, we represent $f(x)$ as a vector based at x; that is, we assign to x the directed line segment from x to $x + f(x)$. For example, if $f(x) = (2x_1^2, x_2)$, then at $x = (1,1)$, we draw an arrow pointing from $(1,1)$ to $(1,1) + (2,1) = (3,2)$. (See Figure 2.1.) Repeating this at every point in a grid covering the plane, we

[1] It is assumed that there is a unique solution.

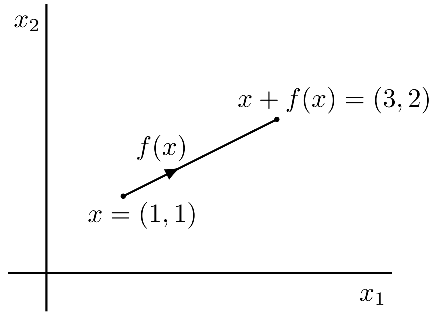

Figure 2.1: Vector field representation.

obtain a *vector field diagram*, such as the one shown in Figure 2.2 for the pendulum equation without friction:

$$\begin{aligned} \dot{x}_1 &= x_2 \\ \dot{x}_2 &= -10 \sin x_1 \end{aligned}$$

In the figure, the length of the arrow at a given point x is proportional to the length of $f(x)$, that is, $\sqrt{f_1^2(x) + f_2^2(x)}$. Sometimes, for convenience, we draw arrows of equal length at all points. Since the vector field at a point is tangent to the trajectory through that point, we can, in essence, construct trajectories from the vector field diagram. Starting at a given initial point x_0, we can construct the trajectory from x_0 by moving along the vector field at x_0. This motion takes us to a new point x_a, where we continue the trajectory along the vector field at x_a. If the process is repeated carefully and the consecutive points are chosen close enough to each other, we can obtain a reasonable approximation of the trajectory through x_0. In the case of Figure 2.2, a careful implementation of the foregoing process would show that the trajectory through $(2, 0)$ is a closed curve.

The family of all trajectories or solution curves is called the *phase portrait* of (2.1)–(2.2). An (approximate) picture of the phase portrait can be constructed by plotting trajectories from a large number of initial states spread all over the x_1–x_2 plane. Since numerical subroutines for solving general nonlinear differential equations are widely available, we can easily construct the phase portrait by using computer simulations. (Some hints are given in Section 2.5.) Note that since the time t is suppressed in a trajectory, it is not possible to recover the solution $(x_1(t), x_2(t))$ associated with a given trajectory. Hence, a trajectory gives only the *qualitative*, but not *quantitative*, behavior of the associated solution. For example, a closed trajectory shows that there is a periodic solution; that is, the system has a sustained oscillation, whereas a shrinking spiral shows a decaying oscillation. In the rest of this chapter, we will qualitatively analyze the behavior of second-order systems by using their phase portraits.

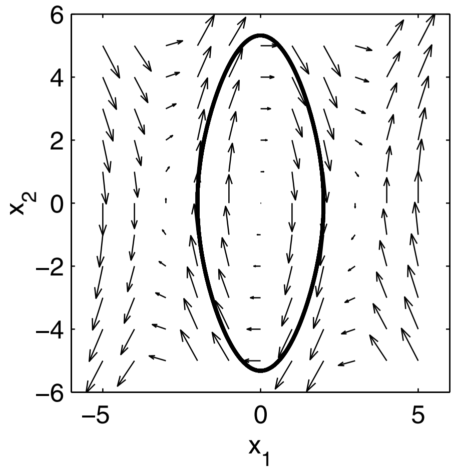

Figure 2.2: Vector field diagram of the pendulum equation without friction.

2.1 Qualitative Behavior of Linear Systems

Consider the linear time-invariant system

$$\dot{x} = Ax \tag{2.3}$$

where A is a 2×2 real matrix. The solution of (2.3) for a given initial state x_0 is given by

$$x(t) = M \exp(J_r t) M^{-1} x_0$$

where J_r is the real Jordan form of A and M is a real nonsingular matrix such that $M^{-1}AM = J_r$. Depending on the eigenvalues of A, the real Jordan form may take one of three forms

$$\begin{bmatrix} \lambda_1 & 0 \\ 0 & \lambda_2 \end{bmatrix}, \quad \begin{bmatrix} \lambda & k \\ 0 & \lambda \end{bmatrix}, \quad \text{and} \quad \begin{bmatrix} \alpha & -\beta \\ \beta & \alpha \end{bmatrix}$$

where k is either 0 or 1. The first form corresponds to the case when the eigenvalues λ_1 and λ_2 are real and distinct, the second form corresponds to the case when the eigenvalues are real and equal, and the third form corresponds to the case of complex eigenvalues $\lambda_{1,2} = \alpha \pm j\beta$. In our analysis, we have to distinguish between these three cases. Moreover, with real eigenvalues, we have to isolate the case when at least one of the eigenvalues is zero. In that situation, the origin is not an isolated equilibrium point and the qualitative behavior is quite different from the behavior in the other cases.

Case 1. Both eigenvalues are real: $\lambda_1 \neq \lambda_2 \neq 0$.

In this case, $M = [v_1, v_2]$, where v_1 and v_2 are the real eigenvectors associated with λ_1 and λ_2. The change of coordinates $z = M^{-1}x$ transforms the system into two decoupled first-order differential equations,

$$\dot{z}_1 = \lambda_1 z_1, \qquad \dot{z}_2 = \lambda_2 z_2$$

whose solution, for a given initial state (z_{10}, z_{20}), is given by

$$z_1(t) = z_{10}e^{\lambda_1 t}, \qquad z_2(t) = z_{20}e^{\lambda_2 t}$$

Eliminating t between the two equations, we obtain

$$z_2 = c z_1^{\lambda_2/\lambda_1} \tag{2.4}$$

where $c = z_{20}/(z_{10})^{\lambda_2/\lambda_1}$. The phase portrait of the system is given by the family of curves generated from (2.4) by allowing the constant c to take arbitrary values in R. The shape of the phase portrait depends on the signs of λ_1 and λ_2.

Consider first the case when both eigenvalues are negative. Without loss of generality, let $\lambda_2 < \lambda_1 < 0$. Here, both exponential terms $e^{\lambda_1 t}$ and $e^{\lambda_2 t}$ tend to zero as $t \to \infty$. Moreover, since $\lambda_2 < \lambda_1 < 0$, the term $e^{\lambda_2 t}$ tends to zero faster than the term $e^{\lambda_1 t}$. Hence, we call λ_2 the fast eigenvalue and λ_1 the slow eigenvalue. For later reference, we call v_2 the fast eigenvector and v_1 the slow eigenvector. The trajectory tends to the origin of the z_1–z_2 plane along the curve of (2.4), which now has a ratio λ_2/λ_1 that is greater than one. The slope of the curve is given by

$$\frac{dz_2}{dz_1} = c\frac{\lambda_2}{\lambda_1} z_1^{[(\lambda_2/\lambda_1)-1]}$$

Since $[(\lambda_2/\lambda_1) - 1]$ is positive, the slope of the curve approaches zero as $|z_1| \to 0$ and approaches ∞ as $|z_1| \to \infty$. Therefore, as the trajectory approaches the origin, it becomes tangent to the z_1-axis; as it approaches ∞, it becomes parallel to the z_2-axis. These observations allow us to sketch the typical family of trajectories shown in Figure 2.3. When transformed back into the x-coordinates, the family of trajectories will have the typical portrait shown in Figure 2.4(a). Note that in the x_1–x_2 plane, the trajectories become tangent to the slow eigenvector v_1 as they approach the origin and parallel to the fast eigenvector v_2 far from the origin. In this situation, the equilibrium point $x = 0$ is called a *stable node*.

When λ_1 and λ_2 are positive, the phase portrait will retain the character of Figure 2.4(a), but with the trajectory directions reversed, since the exponential terms $e^{\lambda_1 t}$ and $e^{\lambda_2 t}$ grow exponentially as t increases. Figure 2.4(b) shows the phase portrait for the case $\lambda_2 > \lambda_1 > 0$. The equilibrium point $x = 0$ is referred to in this instance as an *unstable node*.

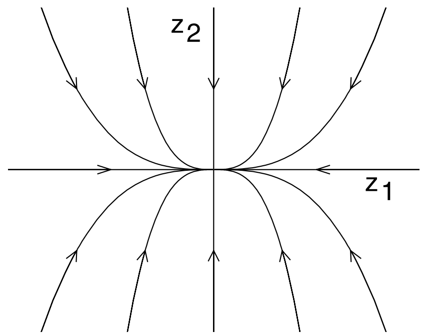

Figure 2.3: Phase portrait of a stable node in modal coordinates.

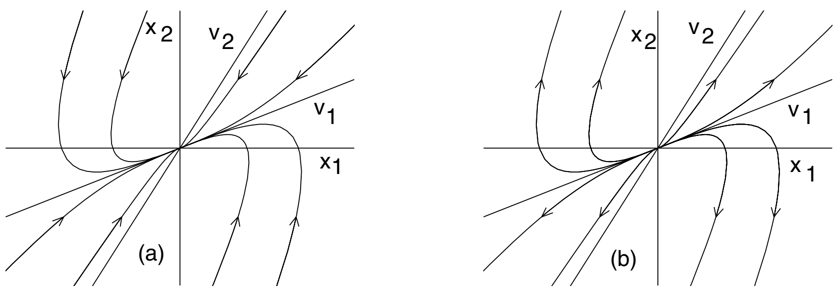

Figure 2.4: Phase portraits for (a) a stable node; (b) an unstable node.

Suppose now that the eigenvalues have opposite signs. In particular, let $\lambda_2 < 0 < \lambda_1$. In this case, $e^{\lambda_1 t} \to \infty$, while $e^{\lambda_2 t} \to 0$ as $t \to \infty$. Hence, we call λ_2 the stable eigenvalue and λ_1 the unstable eigenvalue. Correspondingly, v_2 and v_1 are called the stable and unstable eigenvectors, respectively. Equation (2.4) will have a negative exponent (λ_2/λ_1). Thus, the family of trajectories in the z_1–z_2 plane will take the typical form shown in Figure 2.5(a). Trajectories have hyperbolic shapes. They become tangent to the z_1-axis as $|z_1| \to \infty$ and tangent to the z_2-axis as $|z_1| \to 0$. The only exception to these hyperbolic shapes are the four trajectories along the axes. The two trajectories along the z_2-axis are called the stable trajectories since they approach the origin as $t \to \infty$, while the two trajectories along the z_1-axis are called the unstable trajectories since they approach infinity as $t \to \infty$. The phase portrait in the x_1–x_2 plane is shown in Figure 2.5(b). Here the stable trajectories are along the stable eigenvector v_2 and the unstable trajectories are along the unstable eigenvector v_1. In this case, the equilibrium point is called a *saddle*.

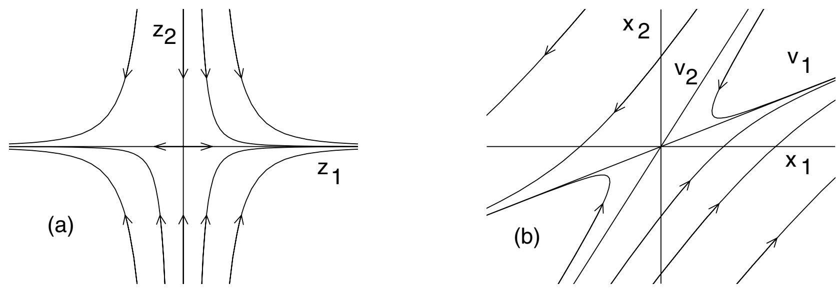

Figure 2.5: Phase portrait of a saddle point (a) in modal coordinates; (b) in original coordinates.

Case 2. Complex eigenvalues: $\lambda_{1,2} = \alpha \pm j\beta$.

The change of coordinates $z = M^{-1}x$ transforms the system (2.3) into the form

$$\dot{z}_1 = \alpha z_1 - \beta z_2, \qquad \dot{z}_2 = \beta z_1 + \alpha z_2$$

The solution of these equations is oscillatory and can be expressed more conveniently in the polar coordinates

$$r = \sqrt{z_1^2 + z_2^2}, \qquad \theta = \tan^{-1}\left(\frac{z_2}{z_1}\right)$$

where we have two uncoupled first-order differential equations:

$$\dot{r} = \alpha r \quad \text{and} \quad \dot{\theta} = \beta$$

The solution for a given initial state (r_0, θ_0) is given by

$$r(t) = r_0 e^{\alpha t} \quad \text{and} \quad \theta(t) = \theta_0 + \beta t$$

which define a logarithmic spiral in the z_1–z_2 plane. Depending on the value of α, the trajectory will take one of the three forms shown in Figure 2.6. When $\alpha < 0$, the spiral converges to the origin; when $\alpha > 0$, it diverges away from the origin. When $\alpha = 0$, the trajectory is a circle of radius r_0. Figure 2.7 shows the trajectories in the x_1–x_2 plane. The equilibrium point $x = 0$ is referred to as a *stable focus* if $\alpha < 0$, *unstable focus* if $\alpha > 0$, and *center* if $\alpha = 0$.

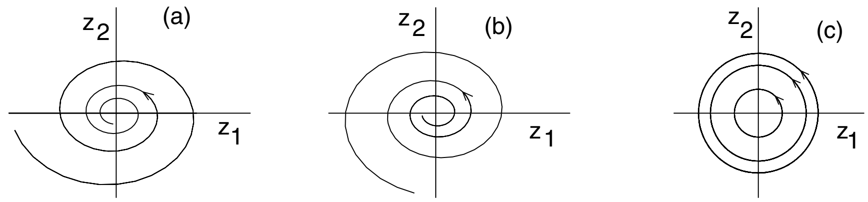

Figure 2.6: Typical trajectories in the case of complex eigenvalues.
(a) $\alpha < 0$; (b) $\alpha > 0$; (c) $\alpha = 0$.

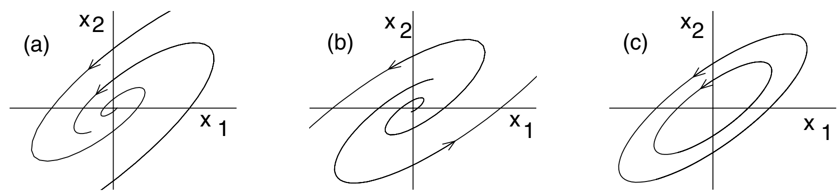

Figure 2.7: Phase portraits for (a) a stable focus; (b) an unstable focus; (c) a center.

Case 3. Nonzero multiple eigenvalues: $\lambda_1 = \lambda_2 = \lambda \neq 0$**.**

The change of coordinates $z = M^{-1}x$ transforms the system (2.3) into the form

$$\dot{z}_1 = \lambda z_1 + k z_2, \qquad \dot{z}_2 = \lambda z_2$$

whose solution, for a given initial state (z_{10}, z_{20}), is given by

$$z_1(t) = e^{\lambda t}(z_{10} + k z_{20} t), \qquad z_2(t) = e^{\lambda t} z_{20}$$

Eliminating t, we obtain the trajectory equation

$$z_1 = z_2 \left[\frac{z_{10}}{z_{20}} + \frac{k}{\lambda} \ln\left(\frac{z_2}{z_{20}} \right) \right]$$

Figure 2.8 shows the form of the trajectories when $k = 0$, while Figure 2.9 shows their form when $k = 1$. The phase portrait has some similarity with the portrait of a node. Therefore, the equilibrium point $x = 0$ is usually referred to as a stable node if $\lambda < 0$ and unstable node if $\lambda > 0$. Note, however, that the phase portraits of Figures 2.8 and 2.9 do not have the asymptotic slow–fast behavior that we saw in Figures 2.3 and 2.4.

Before we discuss the degenerate case when one or both of the eigenvalues are zero, let us summarize our findings about the qualitative behavior of the system when the equilibrium point $x = 0$ is isolated. We have seen that the system can display six qualitatively different phase portraits, which are associated with different

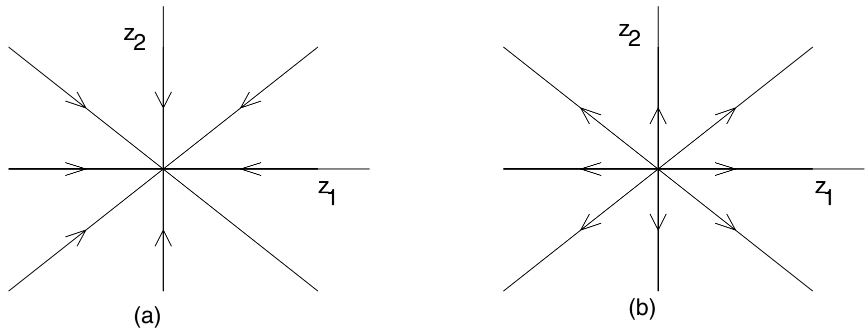

Figure 2.8: Phase portraits for the case of nonzero multiple eigenvalues when $k = 0$: (a) $\lambda < 0$; (b) $\lambda > 0$.

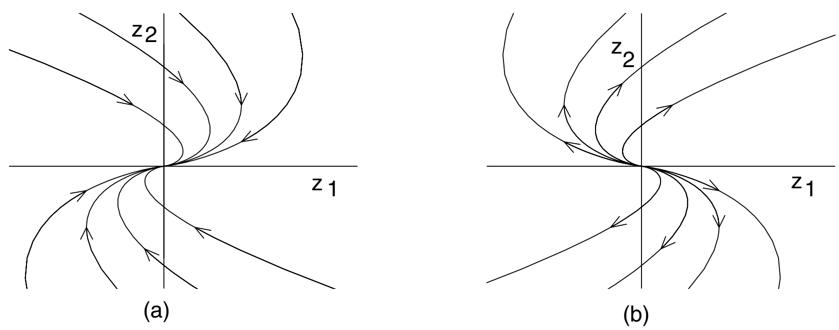

Figure 2.9: Phase portraits for the case of nonzero multiple eigenvalues when $k = 1$: (a) $\lambda < 0$; (b) $\lambda > 0$.

types of equilibria: stable node, unstable node, saddle point, stable focus, unstable focus, and center. The type of equilibrium point is completely specified by the location of the eigenvalues of A. Note that the global (throughout the phase plane) qualitative behavior of the system is determined by the type of equilibrium point. This is a characteristic of linear systems. When we study the qualitative behavior of nonlinear systems in the next section, we shall see that the type of equilibrium point can only determine the qualitative behavior of the trajectories in the vicinity of that point.

Case 4. One or both eigenvalues are zero.

When one or both eigenvalues of A are zero, the phase portrait is in some sense degenerate. Here, the matrix A has a nontrivial null space. Any vector in the null space of A is an equilibrium point for the system; that is, the system has an

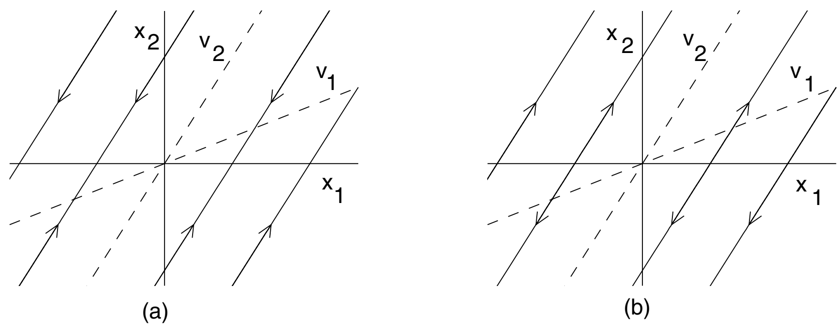

Figure 2.10: Phase portraits for (a) $\lambda_1 = 0,\ \lambda_2 < 0$; (b) $\lambda_1 = 0,\ \lambda_2 > 0$.

equilibrium subspace, rather than an equilibrium point. The dimension of the null space could be one or two; if it is two, the matrix A will be the zero matrix. This is a trivial case where every point in the plane is an equilibrium point. When the dimension of the null space is one, the shape of the Jordan form of A will depend on the multiplicity of the zero eigenvalue. When $\lambda_1 = 0$ and $\lambda_2 \neq 0$, the matrix M is given by $M = [v_1, v_2]$ where v_1 and v_2 are the associated eigenvectors. Note that v_1 spans the null space of A. The change of variables $z = M^{-1}x$ results in

$$\dot{z}_1 = 0, \qquad \dot{z}_2 = \lambda_2 z_2$$

whose solution is

$$z_1(t) = z_{10}, \qquad z_2(t) = z_{20}e^{\lambda_2 t}$$

The exponential term will grow or decay, depending on the sign of λ_2. Figure 2.10 shows the phase portrait in the x_1–x_2 plane. All trajectories converge to the equilibrium subspace when $\lambda_2 < 0$, and diverge away from it when $\lambda_2 > 0$.

When both eigenvalues are at the origin, the change of variables $z = M^{-1}x$ results in

$$\dot{z}_1 = z_2, \qquad \dot{z}_2 = 0$$

whose solution is

$$z_1(t) = z_{10} + z_{20}t, \qquad z_2(t) = z_{20}$$

The term $z_{20}t$ will increase or decrease, depending on the sign of z_{20}. The z_1-axis is the equilibrium subspace. Figure 2.11 shows the phase portrait in the x_1–x_2 plane; the dashed line is the equilibrium subspace. The phase portrait in Figure 2.11 is quite different from that in Figure 2.10. Trajectories starting off the equilibrium subspace move parallel to it.

The study of the behavior of linear systems about the equilibrium point $x = 0$ is important because, in many cases, the local behavior of a nonlinear system near an equilibrium point can be deduced by linearizing the system about that point and

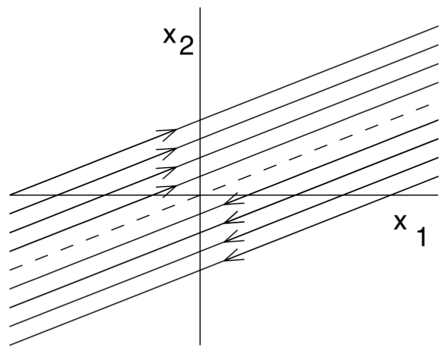

Figure 2.11: Phase portrait when $\lambda_1 = \lambda_2 = 0$.

studying the behavior of the resultant linear system. How conclusive the linearization approach is depends to a great extent on how the various qualitative phase portraits of a linear system persist under perturbations. We can gain insight into the behavior of a linear system under perturbations by examining the special case of linear perturbations. Suppose A has distinct eigenvalues and consider $A + \Delta A$, where ΔA is a 2×2 real matrix whose elements have arbitrarily small magnitudes. From the perturbation theory of matrices,[2] we know that the eigenvalues of a matrix depend continuously on its parameters. This means that, given any positive number ε, there is a corresponding positive number δ such that if the magnitude of the perturbation in each element of A is less than δ, the eigenvalues of the perturbed matrix $A + \Delta A$ will lie in open discs of radius ε centered at the eigenvalues of A. Consequently, any eigenvalue of A that lies in the open right-half plane (positive real part) or in the open left-half plane (negative real part) will remain in its respective half of the plane after arbitrarily small perturbations. On the other hand, eigenvalues on the imaginary axis, when perturbed, might go into either the right-half or the left-half of the plane, since a disc centered on the imaginary axis will extend in both halves no matter how small ε is. Consequently, we can conclude that if the equilibrium point $x = 0$ of $\dot{x} = Ax$ is a node, focus, or saddle point, then the equilibrium point $x = 0$ of $\dot{x} = (A + \Delta A)x$ will be of the same type for sufficiently small perturbations. The situation is quite different if the equilibrium point is a center. Consider the perturbation of the real Jordan form in the case of a center

$$\begin{bmatrix} \mu & 1 \\ -1 & \mu \end{bmatrix}$$

where μ is a perturbation parameter. When μ is positive, the equilibrium point of the perturbed system is an unstable focus; when μ is negative, it is a stable focus.

[2]See [67, Chapter 7].

This is true no matter how small μ is, as long as it is different from zero. Because the phase portraits of a stable focus and unstable focus are qualitatively different from the phase portrait of a center, we see that a center equilibrium point will not persist under perturbations. The node, focus, and saddle equilibrium points are said to be *structurally stable* because they maintain their qualitative behavior under infinitesimally small perturbations,[3] while the center equilibrium point is not structurally stable. The distinction between the two cases is due to the location of the eigenvalues of A, with the eigenvalues on the imaginary axis being vulnerable to perturbations. This brings in the definition of a *hyperbolic equilibrium point.* The origin $x = 0$ is said to be a hyperbolic equilibrium point of $\dot{x} = Ax$ if A has no eigenvalues with zero real part.[4]

When A has multiple nonzero real eigenvalues, infinitesimally small perturbations could result in a pair of complex eigenvalues. Hence, a stable (respectively, unstable) node would either remain a stable (respectively, unstable) node or become a stable (respectively, unstable) focus.

When A has eigenvalues at zero, one would expect perturbations to move these eigenvalues away from zero, resulting in a major change in the phase portrait. It turns out, however, that there is an important difference between the case when there is only one eigenvalue at zero and the case when both eigenvalues are at zero ($A \neq 0$). In the first case, perturbation of the zero eigenvalue results in a real eigenvalue $\lambda_1 = \mu$, where μ could be positive or negative. Since the other eigenvalue λ_2 is different from zero, its perturbation will keep it away from zero. Moreover, since we are talking about arbitrarily small perturbations, $|\lambda_1| = |\mu|$ will be much smaller than $|\lambda_2|$. Thus, we end up with two real distinct eigenvalues, which means that the equilibrium point of the perturbed system will be a node or a saddle point, depending on the signs of λ_2 and μ. This is already an important change in the phase portrait. However, a careful examination of the phase portrait gives more insight into the qualitative behavior of the system. Since $|\lambda_1| \ll |\lambda_2|$, the exponential term $e^{\lambda_2 t}$ will change with t much faster than the exponential term $e^{\lambda_1 t}$, resulting in the typical phase portraits of a node and a saddle shown in Figure 2.12, for the case $\lambda_2 < 0$. Comparing these phase portraits with Figure 2.10(a) shows some similarity. In particular, similar to Figure 2.10, trajectories starting off the eigenvector v_1 converge to that vector along lines (almost) parallel to the eigenvector v_2. As they approach the vector v_1, they become tangent to it and move along it. When $\mu < 0$, the motion along v_1 converges to the origin (stable node), while when $\mu > 0$ the motion along v_1 tends to infinity (saddle point). This qualitative behavior is characteristic of singularly perturbed systems, which will be studied in Chapter 11.

When both eigenvalues of A are zeros, the effect of perturbations is more dra-

---

[3]See [81, Chapter 16] for a rigorous and more general definition of structural stability.

[4]This definition of a hyperbolic equilibrium point extends to higher-dimensional systems. It also carries over to equilibria of nonlinear systems by applying it to the eigenvalues of the linearized system.

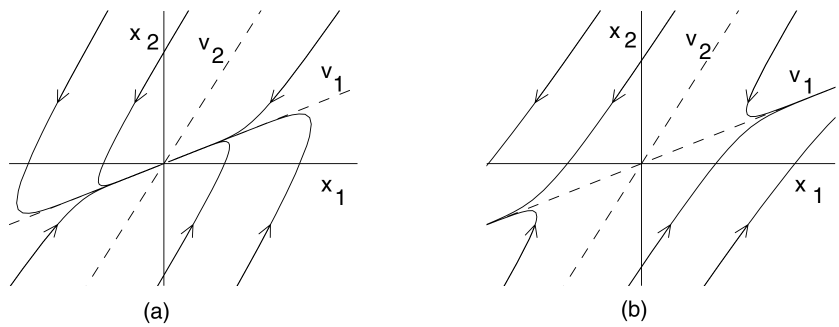

Figure 2.12: Phase portraits of a perturbed system when $\lambda_1 = 0$ and $\lambda_2 < 0$: (a) $\mu < 0$; (b) $\mu > 0$.

matic. Consider the four possible perturbations of the Jordan form

$$\begin{bmatrix} 0 & 1 \\ -\mu^2 & 0 \end{bmatrix}, \quad \begin{bmatrix} \mu & 1 \\ -\mu^2 & \mu \end{bmatrix}, \quad \begin{bmatrix} \mu & 1 \\ 0 & \mu \end{bmatrix}, \quad \text{and} \quad \begin{bmatrix} \mu & 1 \\ 0 & -\mu \end{bmatrix}$$

where μ is a perturbation parameter that could be positive or negative. It can easily be seen that the equilibrium points in these four cases are a center, a focus, a node, and a saddle point, respectively. In other words, all the possible phase portraits of an isolated equilibrium point could result from perturbations.

2.2 Multiple Equilibria

The linear system $\dot{x} = Ax$ has an isolated equilibrium point at $x = 0$ if A has no zero eigenvalues, that is, if $\det A \neq 0$. When $\det A = 0$, the system has a continuum of equilibrium points. These are the only possible equilibria patterns that a linear system may have. A nonlinear system can have multiple isolated equilibrium points. In the following two examples, we explore the qualitative behavior of the tunnel-diode circuit of Section 1.2.2 and the pendulum equation of Section 1.2.1. Both systems exhibit multiple isolated equilibria.

Example 2.1 The state model of a tunnel-diode circuit is given by

$$\begin{aligned} \dot{x}_1 &= \frac{1}{C}[-h(x_1) + x_2] \\ \dot{x}_2 &= \frac{1}{L}[-x_1 - Rx_2 + u] \end{aligned}$$

Assume that the circuit parameters are[5] $u = 1.2\ V$, $R = 1.5\ k\Omega = 1.5 \times 10^3\ \Omega$, $C = 2\ pF = 2 \times 10^{-12}\ F$, and $L = 5\ \mu H = 5 \times 10^{-6}\ H$. Measuring time in

[5]The numerical data are taken from [39].

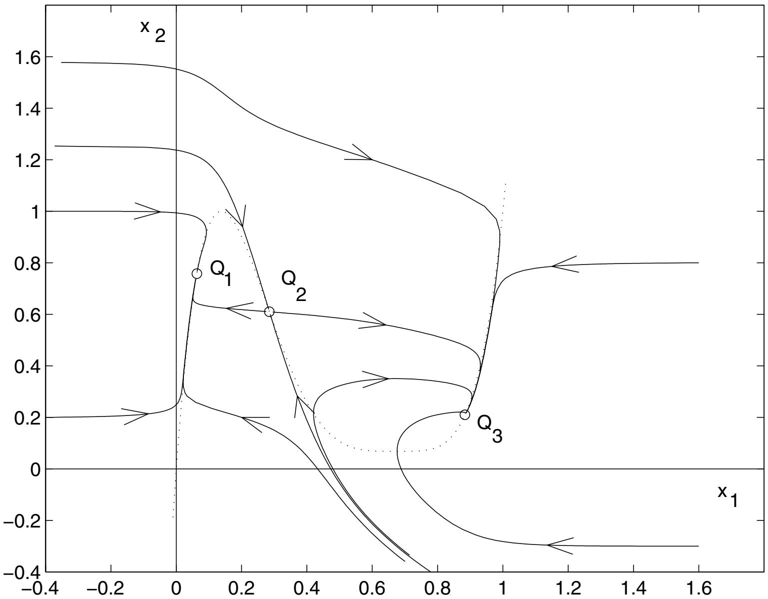

Figure 2.13: Phase portrait of the tunnel-diode circuit of Example 2.1.

nanoseconds and the currents x_2 and $h(x_1)$ in mA, the state model is given by

$$\begin{aligned} \dot{x}_1 &= 0.5[-h(x_1) + x_2] \\ \dot{x}_2 &= 0.2(-x_1 - 1.5x_2 + 1.2) \end{aligned}$$

Suppose that $h(\cdot)$ is given by

$$h(x_1) = 17.76x_1 - 103.79x_1^2 + 229.62x_1^3 - 226.31x_1^4 + 83.72x_1^5$$

By setting $\dot{x}_1 = \dot{x}_2 = 0$ and solving for the equilibrium points, we can verify that there are three equilibrium points at $(0.063, 0.758)$, $(0.285, 0.61)$, and $(0.884, 0.21)$. The phase portrait of the system, generated by a computer program, is shown in Figure 2.13. The three equilibrium points are denoted in the portrait by Q_1, Q_2, and Q_3, respectively. Examination of the phase portrait shows that, except for two special trajectories, which approach Q_2, all trajectories eventually approach either Q_1 or Q_3. Near the equilibrium points, the trajectories take the form of a saddle for Q_2 and stable nodes for Q_1 and Q_3. The two special trajectories, which approach Q_2, are the stable trajectories of the saddle. They form a curve that divides the plane into two halves. All trajectories originating from the left side of the curve will approach Q_1, while all trajectories originating from the right side will approach Q_3. This special curve is called a *separatrix*, because it partitions the

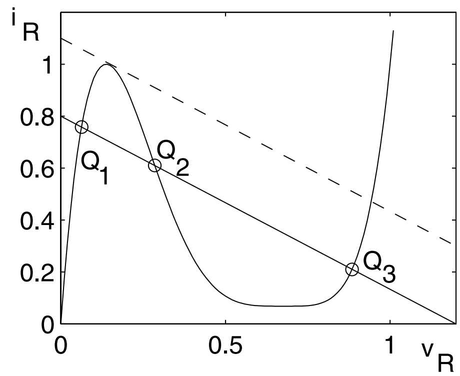

Figure 2.14: Adjustment of the load line of the tunnel-diode circuit during triggering.

plane into two regions of different qualitative behavior.[6] In an experimental setup, we shall observe one of the two steady-state operating points Q_1 or Q_3, depending on the initial capacitor voltage and inductor current. The equilibrium point at Q_2 is never observed in practice because the ever-present physical noise would cause the trajectory to diverge from Q_2 even if it were possible to set up the exact initial conditions corresponding to Q_2.

The phase portrait in Figure 2.13 tells us the global qualitative behavior of the tunnel-diode circuit. The range of x_1 and x_2 was chosen so that all essential qualitative features are displayed. The portrait outside this range does not contain any new qualitative features.

The tunnel-diode circuit with multiple equilibria is referred to as a *bistable* circuit, because it has two steady-state operating points. It has been used as a computer memory, where the equilibrium point Q_1 is associated with the binary state "0" and the equilibrium point Q_3 is associated with the binary state "1." Triggering from Q_1 to Q_3 or vice versa is achieved by a triggering signal of sufficient amplitude and duration that allows the trajectory to move to the other side of the separatrix. For example, if the circuit is initially at Q_1, then a positive pulse added to the supply voltage u will carry the trajectory to the right side of the separatrix. The pulse must be adequate in amplitude to raise the load line beyond the dashed line in Figure 2.14 and long enough to allow the trajectory to reach the right side of the separatrix.

Another feature of this circuit can be revealed if we view it as a system with input $u = E$ and output $y = v_R$. Suppose we start with a small value of u such that the only equilibrium point is Q_1. After a transient period, the system settles at Q_1. Let us now increase u gradually, allowing the circuit to settle at an equilibrium point

[6]In general, the state plane decomposes into a number of regions, within each of which the trajectories may show a different type of behavior. The curves separating these regions are called separatrices.

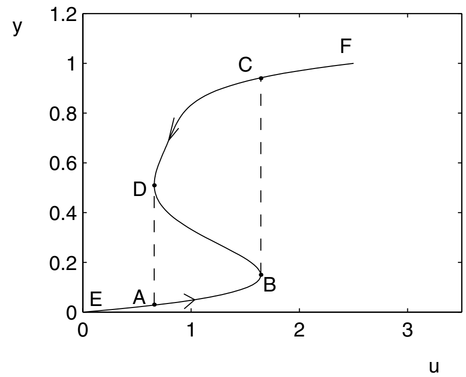

Figure 2.15: Hysteresis characteristics of the tunnel-diode circuit.

after each increment of u. For a range of values of u, Q_1 will be the only equilibrium point. On the input–output characteristic of the system, shown in Figure 2.15, this range corresponds to the segment EA. As the input is increased beyond the point A, the circuit will have two steady-state operating points at Q_1, on the segment AB, and Q_3, on the segment CD. Since we are increasing u gradually, the initial conditions will be near Q_1 and the circuit will settle there. Hence, the output will be on the segment AB. With further increase of u, we will reach a point where the circuit will have only one equilibrium point at Q_3. Therefore, after a transient period the circuit will settle at Q_3. On the input–output characteristic, it will appear as a jump from B to C. For higher values of u, the output will remain on the segment CF. Suppose now that we start decreasing u gradually. First, there will be only one equilibrium point Q_3; that is, the output will move along the segment FC. Beyond a certain value of u, corresponding to the point C, the circuit will have two steady-state operating points at Q_1 and Q_3, but will settle at Q_3 because its initial conditions will be closer to it. Hence, the output will be on the segment CD. Eventually, as we decrease u beyond the value corresponding to D, the circuit will have only one equilibrium point at Q_1 and the characteristic will exhibit another jump from D to A. Thus, the input–output characteristic of the system features a hysteresis behavior. Notice that by drawing the input–output characteristic of Figure 2.15, we ignore the dynamics of the system. Such viewpoint will be reasonable when the input is slowly varying relative to the dynamics of the system so that the transient time between different steady-state operating points can be neglected.[7] △

Example 2.2 Consider the following pendulum equation with friction:

$$\dot{x}_1 = x_2$$

[7]This statement can be justified by the singular perturbation theory presented in Chapter 11.

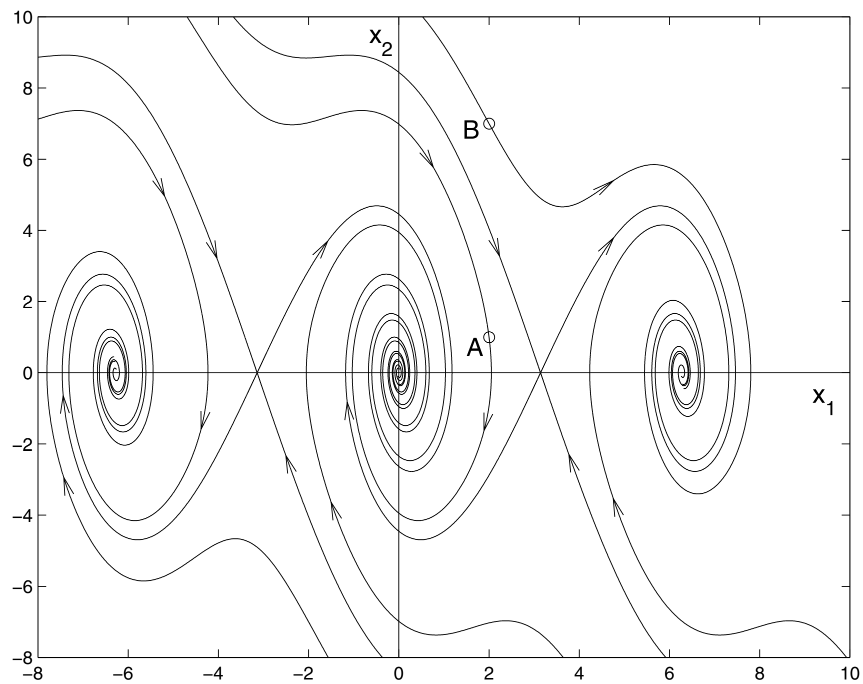

Figure 2.16: Phase portrait of the pendulum equation of Example 2.2.

$$\dot{x}_2 \;=\; -10\sin x_1 - x_2$$

A computer-generated phase portrait is shown in Figure 2.16. The phase portrait is periodic in x_1 with period 2π. Consequently, all distinct features of the system's qualitative behavior can be captured by drawing the portrait in the vertical strip $-\pi \le x_1 \le \pi$. As we noted earlier, the equilibrium points $(0, 0)$, $(2\pi, 0)$, $(-2\pi, 0)$, etc., correspond to the downward equilibrium position $(0, 0)$. Trajectories near these equilibrium points have the pattern of a stable focus. On the other hand, the equilibrium points at $(\pi, 0)$, $(-\pi, 0)$, etc., correspond to the upward equilibrium position $(\pi, 0)$. Trajectories near these equilibrium points have the pattern of a saddle. The stable trajectories of the saddles at $(\pi, 0)$ and $(-\pi, 0)$ form separatrices which contain a region with the property that all trajectories in its interior approach the equilibrium point $(0, 0)$. This picture is repeated periodically. The fact that trajectories could approach different equilibrium points correspond to the number of full swings a trajectory would take before it settles at the downward equilibrium position. For example, the trajectories starting at points A and B have the same initial position, but different speeds. The trajectory starting at A oscillates with decaying amplitude until it settles down at equilibrium. The trajectory starting at B, on the other hand, has more initial kinetic energy. It makes a full swing before it starts to oscillate with decaying amplitude. Once again, notice that the "unstable" equilibrium position $(\pi, 0)$ cannot be maintained in practice, because noise would cause trajectories to diverge away from that position. △

2.3 Qualitative Behavior Near Equilibrium Points

Examination of the phase portraits in Examples 2.1 and 2.2 shows that the qualitative behavior in the vicinity of each equilibrium point looks just like those we saw in Section 2.1 for linear systems. In particular, in Figure 2.13 the trajectories near Q_1, Q_2, and Q_3 are similar to those associated with a stable node, saddle point, and stable node, respectively. Similarly, in Figure 2.16 the trajectories near $(0, 0)$ and $(\pi, 0)$ are similar to those associated with a stable focus and saddle point, respectively. In this section, we will see that we could have seen this behavior near the equilibrium points without drawing the phase portrait. It will follow from the general property that, except for some special cases, the qualitative behavior of a nonlinear system near an equilibrium point can be determined via *linearization* with respect to that point.

Let $p = (p_1, p_2)$ be an equilibrium point of the nonlinear system (2.1)–(2.2) and suppose that the functions f_1 and f_2 are continuously differentiable. Expanding the right-hand side of (2.1)–(2.2) into its Taylor series about the point (p_1, p_2), we obtain

$$\begin{aligned}\dot{x}_1 &= f_1(p_1, p_2) + a_{11}(x_1 - p_1) + a_{12}(x_2 - p_2) + \text{H.O.T.}\\ \dot{x}_2 &= f_2(p_1, p_2) + a_{21}(x_1 - p_1) + a_{22}(x_2 - p_2) + \text{H.O.T.}\end{aligned}$$

where

$$\begin{aligned}a_{11} &= \left.\frac{\partial f_1(x_1, x_2)}{\partial x_1}\right|_{x_1=p_1, x_2=p_2}, &\quad a_{12} &= \left.\frac{\partial f_1(x_1, x_2)}{\partial x_2}\right|_{x_1=p_1, x_2=p_2}\\ a_{21} &= \left.\frac{\partial f_2(x_1, x_2)}{\partial x_1}\right|_{x_1=p_1, x_2=p_2}, &\quad a_{22} &= \left.\frac{\partial f_2(x_1, x_2)}{\partial x_2}\right|_{x_1=p_1, x_2=p_2}\end{aligned}$$

and H.O.T. denotes higher order terms of the expansion, that is, terms of the form $(x_1 - p_1)^2$, $(x_2 - p_2)^2$, $(x_1 - p_1) \times (x_2 - p_2)$, and so on. Since (p_1, p_2) is an equilibrium point, we have

$$f_1(p_1, p_2) = f_2(p_1, p_2) = 0$$

Moreover, since we are interested in the trajectories near (p_1, p_2), we define

$$y_1 = x_1 - p_1 \quad \text{and} \quad y_2 = x_2 - p_2$$

and rewrite the state equations as

$$\begin{aligned}\dot{y}_1 &= \dot{x}_1 = a_{11}y_1 + a_{12}y_2 + \text{H.O.T.}\\ \dot{y}_2 &= \dot{x}_2 = a_{21}y_1 + a_{22}y_2 + \text{H.O.T.}\end{aligned}$$

If we restrict attention to a sufficiently small neighborhood of the equilibrium point such that the higher-order terms are negligible, then we may drop these terms and approximate the nonlinear state equations by the linear state equations

$$\begin{aligned} \dot{y}_1 &= a_{11}y_1 + a_{12}y_2 \\ \dot{y}_2 &= a_{21}y_1 + a_{22}y_2 \end{aligned}$$

Rewriting the equations in a vector form, we obtain

$$\dot{y} = Ay$$

where

$$A = \begin{bmatrix} a_{11} & a_{12} \\ a_{21} & a_{22} \end{bmatrix} = \begin{bmatrix} \frac{\partial f_1}{\partial x_1} & \frac{\partial f_1}{\partial x_2} \\ \frac{\partial f_2}{\partial x_1} & \frac{\partial f_2}{\partial x_2} \end{bmatrix}\Bigg|_{x=p} = \left.\frac{\partial f}{\partial x}\right|_{x=p}$$

The matrix $[\partial f/\partial x]$ is called the Jacobian matrix of $f(x)$, and A is the Jacobian matrix evaluated at the equilibrium point p.

It is reasonable to expect the trajectories of the nonlinear system in a small neighborhood of an equilibrium point to be "close" to the trajectories of its linearization about that point. Indeed, it is true that[8] *if the origin of the linearized state equation is a stable (respectively, unstable) node with distinct eigenvalues, a stable (respectively, unstable) focus, or a saddle point, then, in a small neighborhood of the equilibrium point, the trajectories of the nonlinear state equation will behave like a stable (respectively, unstable) node, a stable (respectively, unstable) focus, or a saddle point*. Consequently, we call an equilibrium point of the nonlinear state equation (2.1)–(2.2) a stable (respectively, unstable) node, a stable (respectively, unstable) focus, or a saddle point if the linearized state equation about the equilibrium point has the same behavior. The type of equilibrium points in Examples 2.1 and 2.2 could have been determined by linearization without the need to construct the global phase portrait of the system.

Example 2.3 The Jacobian matrix of the function $f(x)$ of the tunnel-diode circuit in Example 2.1 is given by

$$\frac{\partial f}{\partial x} = \begin{bmatrix} -0.5h'(x_1) & 0.5 \\ -0.2 & -0.3 \end{bmatrix}$$

where

$$h'(x_1) = \frac{dh}{dx_1} = 17.76 - 207.58x_1 + 688.86x_1^2 - 905.24x_1^3 + 418.6x_1^4$$

[8]The proof of this linearization property can be found in [76]. It is valid under the assumption that $f_1(x_1, x_2)$ and $f_2(x_1, x_2)$ have continuous first partial derivatives in a neighborhood of the equilibrium point (p_1, p_2). A related, but different, linearization result will be proved in Chapter 3 for higher-dimensional systems. (See Theorem 4.7.)